View metadata, citation and similar papers at core.ac.uk
brought to you by CORE
provided by Elsevier - Publisher Connector

Cell
Leading Edge
Review

Revisiting the Central Dogma One Molecule at a Time

Carlos Bustamante,[1,2,3,4,5,*] Wei Cheng,[6,8] and Yara X. Mejia[7,8]
[1]Jason L. Choy Laboratory of Single-Molecule Biophysics
[2]QB3 Institute
[3]Physics Department
[4]Howard Hughes Medical Institute
University of California, Berkeley, CA 94720, USA
[5]Physical Biosciences Division, Lawrence Berkeley National Laboratory, Berkeley, CA 94720, USA
[6]Department of Pharmaceutical Sciences, College of Pharmacy, University of Michigan, 428 Church Street, Ann Arbor, MI 48109, USA
[7]Biological Micro and Nanotechnology, Max Planck Institute for Biophysical Chemistry, Am Faßberg 11, D-37077 Göttingen, Germany
[8]These authors contributed equally to this work
*Correspondence: carlos@alice.berkeley.edu
DOI 10.1016/j.cell.2011.01.033

The faithful relay and timely expression of genetic information depend on specialized molecular machines, many of which function as nucleic acid translocases. The emergence over the last decade of single-molecule fluorescence detection and manipulation techniques with nm and Å resolution and their application to the study of nucleic acid translocases are painting an increasingly sharp picture of the inner workings of these machines, the dynamics and coordination of their moving parts, their thermodynamic efficiency, and the nature of their transient intermediates. Here we present an overview of the main results arrived at by the application of single-molecule methods to the study of the main machines of the central dogma.

Introduction

"The operative industry of Nature is so prolific that machines will be eventually found not only unknown to us but also unimaginable by our mind." So wrote in *De Viscerum Structura* Marcello Malpighi (Malpighi, 1666), the founder of microscopic anatomy. Malpighi (1628–1694), a Professor at the University of Bologna, was the leader of the revolution that swept through the biological sciences in the 17th century and that mirrored the parallel revolution that was occurring in physics. Coincidentally, during the latter, Galileo and Newton refined the concepts of *inertia, force*, and *acceleration* that establish the foundations of kinematics and dynamics and that became the language to describe the operation of machines. Coincidentally again, in both revolutions, the invention of instruments that made it possible to observe and measure what was not directly visible to the human eye, the microscope and the telescope, became the catalyst that unleashed, in both sciences, the modern scientific imagination.

Since the era of Malpighi, the mechanical paradigm has been a recurrent idea in biology. In recent decades, the molecular biology revolution has revealed that much of the inner workings of the cell are the result of specialized units or assembly lines that function as molecular machines (Alberts, 1998). Many of these entities operate as molecular motors, converting chemical energy into mechanical work, and their description must be done in the language of mechanics: "moving parts," forces, torques, displacements, thermodynamic efficiencies, and time. And once again, the recent advent of single-molecule methods, which permit to follow in real-time the individual molecular trajectories without having to synchronize a population of molecules, and specifically the development of single-molecule manipulation, whose direct observables are precisely displacements, forces, and torques, is making it possible to formulate an accurate description of molecular machines and to uncover the physical principles and diverse biological designs that underlie their operation.

Most of these machines are enzymes that couple a thermodynamically spontaneous chemical reaction (typically nucleotide hydrolysis) to a mechanical task. Because of their microscopic dimensions, the many small parts that make up these machine-like devices operate at energies only marginally higher than that of the thermal bath and, hence, their operation is subjected to large fluctuations. The fluctuations revealed by single-molecule analyses are not just a nuance or an artifact of studying them in singulo. In fact, many of them are present and need only be present in very small numbers to carry their physiological role in the cell, a role, therefore, subjected to large fluctuations. Behaving as true thermodynamic open systems, these devices can exchange energy and matter with the bath and take advantage of fluctuations to operate, sometimes, as energy rectifiers. Like "honest" Maxwell Demons that sit astride the line that separates stochastic from deterministic phenomena, the function of these molecular machines is to tame the randomness of molecular events and generate directional processes in the cell.

How does this taming take place? How does this noise affect the coordinated operation required to maintain cellular homeostasis? How should we modify our concepts from macroscopic

chemistry and biochemistry to obtain a more faithful description of these stochastic devices? These and other questions are becoming the common thread that ties the ever-increasing number of single-molecule studies of cellular machines, some of which are the subjects of this Review.

Here we will restrict our review to single-molecule studies of the machinery involved in the metabolism and transactions of nucleic acids, primary protagonists of the central dogma of molecular biology, the operating system of the cell. Processes such as replication, transcription, and translation require the information encoded in the sequence of nucleic acids to be read and copied in a directional manner. Therefore, these machines are all, necessarily, translocases. We have accordingly organized this article following the cell's operational logic. First we will review single-molecule studies of machines involved in the packaging and storage of the genome. This section will be followed by a review of helicases, followed in turn by a review of single-molecule studies of genome replication and DNA transcription, and will end with translation studies.

Translocases in Chromosomal Partitioning and Segregation

Newly replicated DNA molecules must be properly partitioned and segregated into daughter cells, spores, or viral capsids. In many cases, these processes utilize an active mechanism that involves an ATP-dependent translocase. Generally the viral packaging and prokaryotic segregation ATPases belong to the P loop NTPase fold and appear to have an ancient common origin (Catalano, 2005; Iyer et al., 2004b; Koonin et al., 1993). Members of the P loop NTPase fold possess a conserved nucleotide-binding and Mg^{2+}-binding motif (Walker A) and a water-activating motif (Walker B) and belong to one of two major divisions: the KG division, which includes P loop kinases and GTPases, and the ASCE (additional strand conserved E [glutamate]) division. Due to space limitations, we will only review here the main single-molecule results obtained on viral packaging systems.

Viral Packaging Systems

The machinery involved in the packaging of viral DNA has two components, the portal-connector and the ATPase (Catalano, 2005; C.L. Hetherington, J.R. Moffitt, P.J. Jardine, and C.B., unpublished data; Jardine and Anderson, 2006). The phylogenetic origin of these components and their spatial and functional relationships define four different types of viral genome packaging systems: (1) terminase-portal systems, (2) the packaging systems of lipid inner membrane-containing viruses, (3) the φ29-like packaging system, and (4) the adenovirus packaging apparatus (Burroughs et al., 2007). (See Supplemental Information).

Viral DNA packaging has been divided into initiation, elongation, and termination. So far, single-molecule studies have been restricted to bacteriophages T4, lambda, and φ29. The DNA packaging motor of bacteriophage φ29, the best studied so far, is made up of three concentric rings (Grimes et al., 2002) (Figure 1A): (1) the head–tail connector, a dodecamer that fits in the pentameric opening at one of the ends of the capsid; (2) a ring of five molecules of RNA, each 174 nucleotides (nt) long of unknown function; and (3) a pentameric ring (Morais et al., 2008) of gp16, an ATPase that belongs to the FtsK/HerA family of the ASCE superfamily of P loop NTPases.

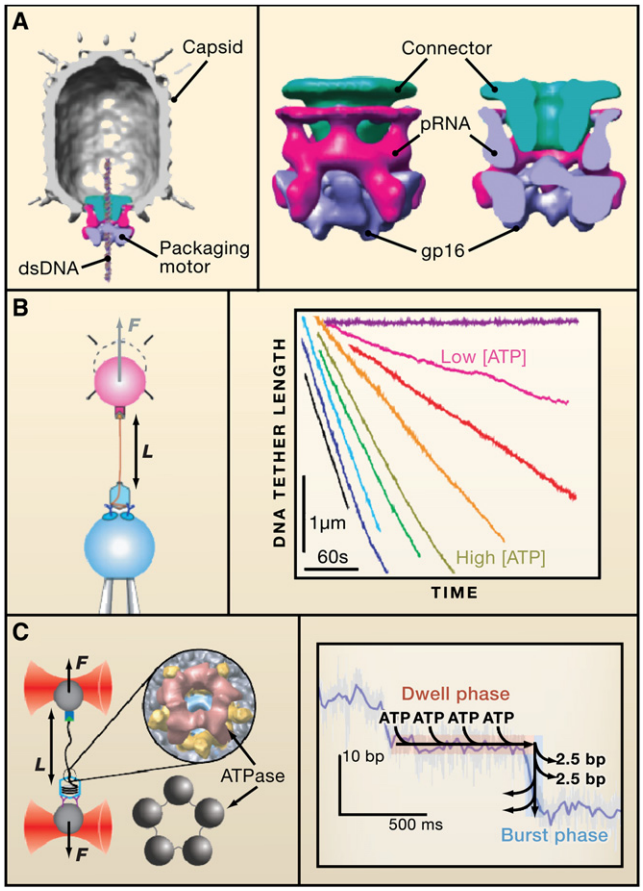

Figure 1. φ29 Packaging Motor

(A) Cryo-electron microscopy of the packaging motor. Left: Packaging motor with capsid and DNA modeled in for scale. Right: Close-up on packaging motor. Modified from Morais et al. (2008).

(B) Optical tweezers packaging assay. Left: An optical trap exerts a force, *F*, on a single packaging bacteriophage while monitoring the length, *L*, of the unpackaged DNA. Right: DNA length versus time. Different colors correspond to different concentrations of [ATP].

(C) High-resolution packaging reveals a burst-dwell packaging mechanism. Left: Cartoon layout of high-resolution packaging assay. Right: Schematic diagram of the kinetic events that occur during the dwell and burst phases overlaid on packaging data.

Packaging Initiation

Initiation of viral DNA packaging requires recognition of the viral genome by the packaging machinery. This process is done either through binding of a specific DNA sequence (reviewed in Catalano, 2005; Jardine and Anderson, 2006) or through a terminal protein bound to the ends of the viral DNA. Only the latter form of initiation has been studied by single-molecule methods. In bacteriophage φ29, a terminal protein, gp3, is bound to both 5′ ends of the viral genome, and at least one of them is required for robust packaging in vitro. In EM studies, the terminal protein is seen to induce a loop or lariat on the

Box 1. Basics of Optical Tweezers

Optical tweezers are a means of exerting forces on objects and to measure those forces. Optical tweezers can be built by focusing a laser beam through a positive lens to form a "trap." The interaction of small dielectric objects with a focused Gaussian beam generates a force in the direction of the field gradient that draws it toward the center of the beam and traps it there. A restoring force arises whenever the object is displaced away from the center of the beam (left inset). When the size of the object is greater than the wavelength of the light (a cell, a plastic bead), this restoring or trapping force can be seen to arise from the exchange of linear momentum of the light with the object in its path and can be understood from geometric ray tracing optics (left inset). Photons carry momentum; when the object is removed from the center of the beam it deflects the beam producing a rate of change of momentum in the light, i.e., a force. Because of the conservation of momentum, the object must experience also a rate of change of momentum, or a force of equal but opposite magnitude that tends to restore the object back to the center of the beam. This restoring force can be measured directly by projecting the beam onto a position-sensitive photo-detector and measuring both its intensity and its deflection. It is typically in the range of 1 to 200 piconewton (pN) depending on the intensity of the beam, a force range sufficient to break the majority of noncovalent interactions involved in most macromolecular interactions and sufficient to stall most molecular motors. For example, the stall force of myosin is between 3–5 pN (Finer et al., 1994), whereas that of kinesin is ~7 pN under saturating [ATP] (Visscher et al., 1999). Because this restoring force is proportional to the stiffness of the trap and to the displacement Δx of the object from the center of the trap, the force can also be determined from this displacement using Hooke's law: $F = k\Delta x$ (right inset). Forces can be applied to molecules by attaching them to the surface of a micron-size optically trapped polystyrene bead through complementary biochemistry.

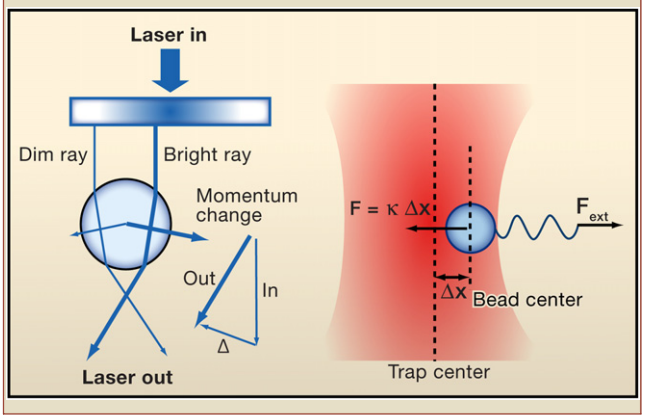

DNA that appears to be supercoiled by the packaging machinery (Grimes and Anderson, 1997b) and that is thought to be necessary for initiation (Grimes and Anderson, 1997a; Koti et al., 2008; Turnquist et al., 1992). Optical tweezers experiments (Box 1) in which DNA packaging is initiated in situ suggest that DNA recognition by the packaging machinery leads to the formation of some kind of loop structure that can be packaged (Rickgauer et al., 2006). Packaging initiation of DNA without the terminally bound gp3 has been observed in optical tweezers experiments, albeit with low efficiency and without affecting translocation (Rickgauer et al., 2006), suggesting that the protein role is circumscribed to assist the search phase of initiation.

Packaging Elongation

Viral DNA packaging involves translocation of DNA by the multimeric ring ATPases through the portal-connector structure into the capsid. Single-molecule studies of viral DNA packaging have used an experimental design as shown in Figure 1B. Here a tether is formed between a packaging viral capsid bound to the surface of a bead and the distal end of the DNA bound to another bead and usually held in an optical trap (Chemla et al., 2005; Fuller et al., 2007a, 2007b; Smith et al., 2001).

These types of studies revealed that the φ29 motor is capable of producing forces as high as 60 piconewton (pN), corresponding to an internal pressure of DNA inside the capsid at the end of packaging of ~6 MPa or 60 atm (Smith et al., 2001). Similar forces have been reported for T4 (Fuller et al., 2007a) and for lambda (Fuller et al., 2007b). It is likely, however, that the motor is capable of generating higher forces and that those measured are *operational* stall forces at which the motor is forced to enter an off-pathway inactive state through structural deformation or unfolding, for example.

In a molecular motor, force is itself a product of the reaction. Moreover, the step in which the conversion from chemical to mechanical energy occurs is the one where movement is generated and must be sensitive to external force. External force can thus be used as an inhibitor of the reaction: by varying its magnitude as a function of ATP concentration, above and below its Michaelis-Menten constant (K_M), we can determine in what step of the hydrolysis cycle the mechano-chemical conversion occurs (Keller and Bustamante, 2000). In φ29 the power stroke of the ATPases coincides with the release of the inorganic phosphate from ATP hydrolysis (Chemla et al., 2005).

The rate of viral DNA packaging varies among different systems. For φ29 under saturating ATP concentrations, it has a narrow distribution around 120 bp/s (Chemla et al., 2005), whereas it is highly variable for T4 reaching values as high as 2000 bp/s, with an average of ~700 bp/s. Interestingly, this variation is observed among viral particles (*static dispersion*) and at different times for the same particle (*dynamic dispersion*) (Fuller et al., 2007a). The latter observations suggest that the motor can interconvert between alternative different functional states within the duration of the single-molecule assay (Fuller et al., 2007a).

Resolving the Individual Steps of a Packaging Motor

For φ29, it was found that the activities of the ATPases around the ring are strictly coordinated into an overall motor's cycle, as addition of small amounts of nonhydrolyzable ATP analogs pauses the motor for variable periods that, presumably, correspond to the times required by the ATPases to exchange their nonhydrolyzable substrate for ATP. The pause density (number of pauses per unit length of DNA packaged) increases linearly with the concentration of analog, indicating that a single bound analog is sufficient to stop the motor (Chemla et al., 2005). The first direct characterization of the intersubunit coordination and the step size of a ring ATPase were reported recently for φ29. Using ultra-high-resolution optical tweezers (Moffitt et al.,

2006), it was found that this motor packages the DNA in increments of 10 bp separated by stochastically varying dwell times (Moffitt et al., 2009). Statistical analysis of the dwell times revealed that multiple ATPs bind during each dwell; application of high force showed that these 10 bp increments are composed of four 2.5 bp steps. Further analysis demonstrated that the hydrolysis cycles of the individual subunits are highly coordinated: the ATP binding to all subunits occurs during the "dwell" phase that is completely segregated from and followed by the translocation or "burst" phase (Figure 1C). Interestingly, the strong coordination among the ATPase activities in the ring is not consistent with the Hill coefficient of ~1 measured experimentally. It turns out that if the binding of the individual ATPs to the various subunits is separated by an irreversible step, the Hill analysis will yield n = 1 despite the strong coordination and cooperativity among these subunits (Moffitt et al., 2009).

The Nature of the DNA-Motor Interaction

Little is known about the interactions responsible for the large forces displayed by these motors and the noninteger base pair steps observed for φ29. The role played by the phosphate backbone charge in the motor-DNA interaction was investigated recently in single-molecule packaging experiments by challenging the motor with DNA constructs bearing inserted regions of neutral DNA segments containing methylphosphonate (MeP) modifications (Aathavan et al., 2009). Remarkably, the motor actively traverses these inserts, though with reduced probability compared to regular DNA, indicating that phosphate charges are important but not essential for translocation. By changing the length of the MeP inserts and selectively restoring the charge to one or the other DNA strand, it was found that important contacts are made with phosphate charges every 10 bp on the 5′→3′ strand only. High-resolution measurements of the dynamics through the insert reveal that, in addition to providing a load-bearing contact, these phosphate contacts also play a role regulating the timing of the mechanochemical cycle (Aathavan et al., 2009).

A step size that is a noninteger number of base pairs requires motor-DNA interactions that do not depend on any given periodic structure in the DNA molecule, and that are of steric nature. Thus, the motor was challenged with a series of additional inserts: DNA lacking bases and sugars, single-stranded gaps, unpaired bulges, and a nonbiological linker (Aathavan et al., 2009). Surprisingly, none of the modifications abolish packaging, indicating that the motor makes promiscuous, steric contacts with a wide variety of chemical moieties over a range of geometries, helping to rationalize the observed 2.5 Å steps. These results suggest that the 2.5 bp step is determined by the magnitude of the conformational change that the individual ATPases undergo during their power stroke.

The Structural Basis of Force Generation

Several sequence motifs define the members of the ASCE family of P loop NTPases (Erzberger and Berger, 2006; Iyer et al., 2004a; Thomsen and Berger, 2008), including the Walker A and Walker B motifs—known to coordinate binding of the nucleotides and to catalyze hydrolysis (Dhar and Feiss, 2005) —and the arginine finger. In addition, the Q-motif and the C-motif are present in some of the packaging ATPases (Mitchell et al., 2002; Rao and Feiss, 2008). These conserved sequence elements are likely to be involved in the mechanochemical energy transduction of viral packaging machines and are, therefore, prime targets for combined mutational and single-molecule studies. Tsay et al. (2009) used optical tweezers to investigate the effect of mutations in the large terminase subunit of bacteriophage λ on the dynamics of packaging. One of the mutations, K84A, near the Walker A motif reduced packaging velocity by ~40% but did not affect the processivity of the motor nor its force sensitivity (i.e., the distance to the transition state) (see Supplemental Information). The other mutant, Y46F, was found to reduce the rate of the motor by ~40% but to decrease also its processivity 10-fold. This same mutant greatly weakened the motor mechanically (Tsay et al., 2009). These findings indicate that viral motors contain an adenine-binding motif that regulates ATP hydrolysis and substrate affinity analogous to the Q-motif recently identified in DEAD-box RNA helicases. Furthermore, the Q-motif appears to be involved in coupling the conformational changes in the ATP-binding pocket to substrate translocation (Worrall et al., 2008). In a separate study, Tsay et al. (2010) found that mutation T194M downstream of the Walker B motif slows the motor 8-fold without modifying its processivity or force generation. In contrast, mutation G212S in the C-motif causes a 3-fold reduction in velocity but also a 6-fold reduction in processivity. Future studies using Å-resolution optical tweezers should help establish which phase of the dynamic cycle of the motor, relative to nucleotide binding and hydrolysis, is directly affected by these modifications.

Helicases: Keys to the Sequence Vault

Helicases constitute a large class of motor proteins that play indispensible roles in almost every aspect of nucleic acid metabolism (Matson et al., 1994; Rocak and Linder, 2004). Most organisms encode multiple helicases, and genes encoding proteins with helicase/translocase activities comprise close to 2% of the eukaryotic genome (Shiratori et al., 1999). Conventionally, helicases are defined as enzymes that utilize ATP to break the complementary hydrogen bonds in double-stranded nucleic acids (dsNA), a process essential for DNA or RNA replication (Lohman and Bjornson, 1996). Biochemical functions of helicases go beyond the mere catalytic opening of double-stranded DNA (dsDNA) or RNA (dsRNA), however. Many helicases not only perform canonical functions but also catalyze disassembly of protein-nucleic acid complexes (PNAC), an important activity required in many essential cellular processes (Jankowsky and Bowers, 2006; Krejci et al., 2003). In addition, some helicase proteins may not function to unwind dsNA but rather serve other biological functions inside the cell, like chromatin remodeling (Saha et al., 2006). This multifunctional facet begs important questions about helicases: How do helicases use ATP to catalyze the opening of dsDNA or the disassembly of PNAC? How are these activities integrated in a given molecule? How is ATP hydrolysis coordinated with the mechanical tasks of the enzyme? Research over the last 10 years, often using single-molecule techniques, has yielded a tremendous amount of information at a mechanistic level on how these proteins catalyze the opening of dsNA and the disassembly of PNAC. These advances will be reviewed here.

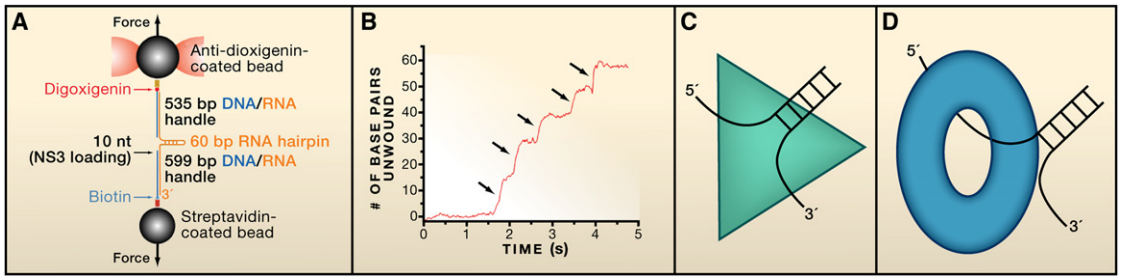

Figure 2. Single-Molecule Studies of Helicases and Mechanistic Insights

(A) Single-molecule hairpin assay for NS3 helicase: cartoon representation of the experimental setup using optical tweezers to study translocation and unwinding of double-stranded RNA by individual NS3 helicase.

(B) Representative real-time unwinding trajectory of NS3 helicase on the hairpin substrate collected at 1 mM ATP; the burst of NS3 activity is noted by arrows and has an average size of 11 ± 3 bp.

(C) Possible mode of binding in NS3 helicase. The binding of 3′ single strand is observed in cocrystal structures between NS3 and single-stranded nucleic acids. However, the binding of 5′ single strand has not been observed in any crystal structures but is suggested from single-molecule studies.

(D) Hexameric helicase, for example, T7 gp4 DNA helicase, extrudes one strand of the DNA through the center hole of the helicase while displacing the other strand.

Common Structural Features of Helicase Proteins

Although helicases are functionally diverse, their protein sequences and three-dimensional (3D) structures have several common features (Supplemental Information). All helicases appear to have common structural building blocks (Bird et al., 1998; Story et al., 1992; Waksman et al., 2000). However, despite this similarity, two classes of helicases have been long recognized, based on their oligomeric structures. One class forms characteristic rings, typically hexameric, and helicase activity appears to require formation of the hexamer (Patel and Picha, 2000). The second class comprises a large number of helicases, mainly grouped in the SF1 and SF2 superfamilies (Gorbalenya and Koonin, 1993), that do not form hexameric structures, although many of them still undergo oligomerization reactions (Lohman and Bjornson, 1996) (Supplemental Information).

Helicase-Catalyzed dsNA Unwinding

How do these motor proteins couple ATP binding and hydrolysis to the mechanical function of strand separation in dsNA? Extensive biochemical and biophysical studies have been carried out on several model helicases in order to answer this question (Lohman et al., 2008; Mackintosh and Raney, 2006; Myong and Ha, 2010; Patel and Picha, 2000; Pyle, 2008). One of the best characterized nonhexameric helicases is the NS3 protein from hepatitis C virus (HCV) (Kolykhalov et al., 2000), a representative member of Superfamily 2 (Gorbalenya and Koonin, 1993), possessing structural resemblance to other helicase proteins despite an overall low sequence identity beyond the helicase motifs (Korolev et al., 1998) (Figure S1). Although its exact biological function is still not clear (Lindenbach and Rice, 2005; Moradpour et al., 2007), this helicase is essential for viral RNA replication and virion assembly (Lam and Frick, 2006; Ma et al., 2008), and as such, it is a potentially important drug target (Frick, 2003; Raney et al., 2010). It displays both DNA (Pang et al., 2002) and RNA helicase activities in vitro. Although dimerization enhances its RNA helicase processivity in vitro (Serebrov and Pyle, 2004), the NS3 protein monomer possesses helicase activity by itself (Cheng et al., 2007; Jennings et al., 2009; Serebrov et al., 2009).

Single-molecule experiments have been particularly useful for revealing molecular mechanisms underlying the operation of helicases (Bianco et al., 2001; Bustamante et al., 2000; Dohoney and Gelles, 2001; Ha et al., 2002). In particular, optical tweezers have been used to follow for the first time the individual trajectories of single NS3 molecules powered by ATP (Dumont et al., 2006). Shown in Figure 2A is a schematic representation of the experimental set up used to monitor the unwinding activity of individual molecules of NS3 on dsRNA (Cheng et al., 2007; Dumont et al., 2006). A single RNA hairpin molecule was attached between a microsphere in an optical trap and a microsphere placed atop a micropipette via hybrid RNA-DNA "molecular handles" to separate the hairpin from the surfaces. The RNA substrate contains a 3′ single-stranded RNA (ssRNA) "launching pad" 10 nt long that facilitates loading and initiation of NS3 helicase activity (see Supplemental Information for polarity of helicase unwinding). NS3 and ATP are next added together into the chamber, while the tethered RNA substrate is held at a constant tension at a preset value, below the mechanical unfolding force of the hairpin. As NS3 unwinds the hairpin, the molecule lengthens, requiring the beads to be separated to maintain the force constant. The end-to-end distance of the molecule can be converted to the number of RNA bp unwound by using the worm-like chain model of ssRNA elasticity (Bustamante et al., 1994) (Box 2), yielding traces with ~2 bp spatial resolution and 20 ms time resolution. Several lines of evidence suggest that the functional form of NS3, observed in this single-molecule experiment, is a monomer (Dumont et al., 2006).

Typical unwinding trajectories consist of cycles of bursts of base pair-opening activity followed by pauses (Figure 2B). The average size of these bursts is 11 ± 3 bp, or about the pitch of dsRNA. The length of the pauses between these 11 bp steps, like the velocity within the 11 bp steps, is [ATP] dependent. These 11 bp steps further decompose into smaller "substeps" at low [ATP], with an average substep size of 3.6 ± 1.3 bp at 50 μM ATP. Dwell time analysis further implies that one ATP is bound during the pause, and one ATP is bound before every substep. However, the 3.6 bp may not represent the minimal

Box 2. Worm-like Chain Model of Polymer Elasticity

Although the rates of nucleic acid translocases are expressed in base pairs per second (bp/s) or nucleotides per second, in many single-molecule manipulation experiments of translocases, the quantity measured is change in time of the end-to-end distance of the nucleic acid at some force. It is thus necessary to convert this distance into molecular contour length, and this, in turn, into numbers of base pairs or nucleotides. The worm-like chain model of DNA elasticity (Bustamante et al., 1994) describes correctly the elastic response of single DNA molecules (Smith et al., 1992, 1996). The expression derived from this model (see Equation 1) relates the end-to-end distance extension (x) of a polymer molecule to its contour length (L) at a given external force (F) applied at its ends. For double-stranded DNA, the contour length of the DNA is the unit length of a single base pair (0.34 nm for standard B-form DNA) times the number of base pairs (k_B, Boltzmann constant; T, absolute temperature; and P, the persistence length of the polymer).

$$\frac{FP}{k_B T} = \frac{1}{4(1 - x/L)^2} + \frac{x}{L} - \frac{1}{4} \quad (1)$$

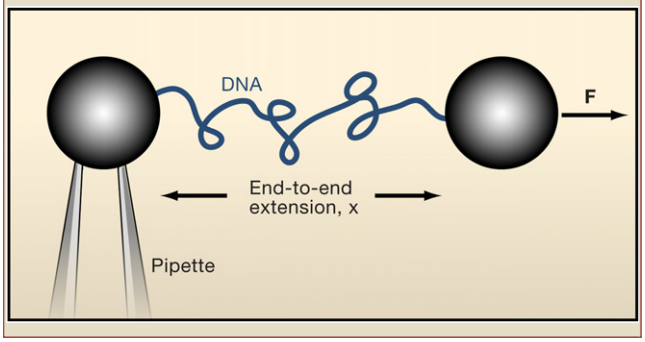

Box 3. Basics of Magnetic Tweezers

Magnetic tweezers use an external magnetic field to exert forces on macromolecules attached to micron-size paramagnetic beads via complementary biochemistry. Limited by the magnetic field strength, the range of force that can be applied by magnetic tweezers is typically one order of magnitude lower than that in optical tweezers (1 to 10 pN). However, magnetic tweezers can hold this force constant with sub-piconewton precision for a remarkable length of time. In addition, because the magnetic field is not localized to a single spot in space, as is the case with most optical tweezers, magnetic tweezers can be used to manipulate simultaneously many molecules in parallel, thus increasing the throughput of experiments. Moreover, because most magnetic beads have a small permanent magnetization, an external rotating magnetic field can be used to introduce torsion and supercoil DNA (Strick et al., 1996; Bryant et al., 2003).

step of the enzyme due to limitations in spatial and temporal resolution of the experiment. The 11 bp steps separated by pauses, and their decomposition into smaller substeps, were rationalized through an inchworm mechanism that requires at least two separate RNA-binding sites in NS3 (Dumont et al., 2006).

The force on the hairpin was found to strongly enhance NS3 processivity but did not affect pause duration or stepping velocity. The processivity of a helicase (Lohman et al., 1998) measures the relative probability that the enzyme remains bound to the nucleic acid instead of detaching: $p = k_{forward}/(k_{forward} + k_{off})$, where $k_{forward}$ is the rate constant of forward movement and k_{off} is the rate of helicase dissociation. Because $k_{forward}$ does not change with force, the increase of helicase processivity must be due to a decrease of its k_{off}. This explanation is consistent with crystal structures of NS3 in complex with ssRNA, in which the flexible ssRNA adopts an extended form in the NS3-binding site (Appleby et al., 2010). Presumably, force helps overcome the configurational entropy loss associated with chain stretching, decreasing the off rate. The invariance of $k_{forward}$ with force also suggests that either strand separation by NS3 is not rate limiting in the reaction or that the dsRNA at the junction is protected by NS3 from being directly acted on by mechanical force. A subsequent study in which RNA hairpins harboring different sequences were used (Cheng et al., 2007) favors the second explanation. This study revealed that pause duration and stepping rate are strongly influenced by the base pair sequence, i.e., by the magnitude of the barrier at the fork, and indicates that the force insensitivity of the stepping velocity is more likely due to junction protection by the enzyme. Surprisingly, this study found that regions of high duplex stability ahead of the junction lead to increased NS3 dissociation and reduced processivity. These authors proposed a mechanism in which the enzyme contacts the duplex as far as 6 bp ahead of the junction and destabilizes it to start a new inchworm cycle. A stable duplex ahead of the junction can induce enzyme dissociation (Cheng et al., 2007).

The independence of unwinding rate and the increase of processivity with the external force applied to the hairpin were similarly observed in a single-molecule magnetic tweezers (Box 3) study of *E. coli* DNA helicase UvrD, a 3′ to 5′ nonhexameric DNA helicase with structural resemblance to NS3 (Dessinges et al., 2004).

Recent pre-steady-state bulk kinetic studies have confirmed the 11 bp step size for NS3 monomer (Serebrov et al., 2009). Interestingly, a single-molecule fluorescence (Box 4) study on NS3 catalyzing the opening of dsDNA did not reveal the 11 bp stepping seen both in optical tweezers and in pre-steady-state bulk experiments. This study found instead a periodic 3 bp step size for the helicase (Myong et al., 2007). Analysis of the pauses separating the 3 bp steps suggests that there are three rate-limiting events within each 3 bp step, although whether the rate-limiting events correspond to single bp steps remains to be addressed.

A similar single-molecule optical tweezers assay was developed for bacteriophage T7 hexameric helicase (Johnson et al., 2007). Both the processivity and unwinding rate of the helicase increase with the application of mechanical force at hairpin ends; the ring in hexameric helicases can open (Ahnert et al., 2000), which may allow them to detach from the nucleic acids. The unwinding rate of the helicase also varies with the DNA sequence. Theoretical analysis of the unwinding rates from this study supports an active mechanism in which the helicase preferentially stabilizes the open over the closed form of the

Box 4. Basics of Single-Molecule Fluorescence

The ability to detect the fluorescence emitted by certain dyes at the single-molecule level has furnished another way to follow the dynamics of complex biochemical processes in real-time. Single-molecule fluorescence methods make it possible, for example, to localize the emitter with nanometer precision (Yildiz et al., 2003). In particular, single-molecule fluorescence resonance energy transfer, FRET, takes advantage of the fact that the fluorescence emission of a molecule (called a donor) is influenced by a neighboring molecule (the acceptor) through dipolar coupling. The efficiency of this coupling is determined by the spectral overlap between the emission of the donor and the absorbance of the acceptor, the distance, and the orientation between these two molecules. Because this efficiency decreases with the sixth power of the distance between the donor and the acceptor, this method can be used to monitor conformational changes of macromolecules or changes in the relative orientation between macromolecules. In practice, FRET is better used to monitor relative changes in distance and/or orientation because the absolute distance measurements require information about the orientation of the fluorophores, which is not always available (Muschielok et al., 2008). The application of single-molecule fluorescence techniques to nucleic acid translocases has revealed many novel insights and mechanistic details of these motors (Ha et al., 2002). These experiments are mostly carried out using evanescent field excitation to reduce fluorescence background and achieve single-molecule sensitivity. This particular experimental design also permits to monitor many individual molecules simultaneously.

junction (Betterton and Julicher, 2005) (see Supplemental Information for passive versus active unwinding). Although not directly observed in this study, the analysis of unwinding rates indicates a step size of 2 bp. Using a magnetic tweezers assay, Lionnet et al. studied the DNA-unwinding mechanism catalyzed by bacteriophage T4 helicase gp41, a hexameric helicase involved in phage DNA replication (Lionnet et al., 2007). The difference between the rate of unwinding in these experiments (30 bp/s) and the expected rate in vivo (400 bp/s) suggests that gp41 must interact with other components of the replisome to achieve rapid and processive unwinding of the T4 genome. Interestingly, this study showed a clear dependence of DNA-unwinding rate on the tension applied to the hairpin.

Hexameric versus Nonhexameric Helicases

A comparison of the behavior of hexameric and nonhexameric helicases reveals that for both groups processivity increases with applied force and the rate of dsNA unwinding depends on the thermodynamic stability of the base pair at the junction. However, the unwinding rate of nonhexameric helicases is insensitive to mechanical force on the hairpin (Dessinges et al., 2004; Dumont et al., 2006), whereas that of hexameric helicases studied so far increases with force (Johnson et al., 2007; Lionnet et al., 2007). The speeding up of hexameric helicases with force indicates that strand separation constitutes the rate-limiting step of their mechanochemical cycle. It also suggests that these two classes of helicases may interact with their dsNA substrates in different ways: whereas nonhexameric helicases may protect the junction and hold onto the single-stranded nucleic acids (ssNA) chains immediately after separation, preventing the force to reach the junction (Figure 2C), hexameric helicases do not protect the junction (Figure 2D). Structural (Enemark and Joshua-Tor, 2008) and biochemical studies (Patel and Picha, 2000) have shown that ring-shaped helicases pass one strand of the dsDNA through the center channel of the ring while excluding the other strand, consistent with a simple picture of a "wire stripper" (Figure 2D). In contrast, single-molecule fluorescence studies on NS3 suggest that the helicase maintains contact with the 5′ displaced single strand during unwinding (Myong et al., 2007). This notion is supported by the observation that domain II of the protein contains a positive patch that may form part of the exit path for the displaced 5′ single strand (Serebrov et al., 2009).

Protein-Displacement Activity of Helicases

Although genetic studies have long implied the role of helicases in DNA recombination and repair (Aboussekhra et al., 1992; Palladino and Klein, 1992), it was not until recently that biochemical studies demonstrated unambiguously their requirement for disassembly of the DNA-Rad51 complex, the recombination intermediate in eukaryotes (Krejci et al., 2003; Veaute et al., 2003). Helicase malfunction in this case leads to hyperrecombination and cell death (Gangloff et al., 2000). There are also numerous examples of the involvement of RNA helicases in disassembly of RNA-protein complexes (Jankowsky and Bowers, 2006).

The mechanisms by which helicases catalyze protein displacement are just beginning to be explored (Antony et al., 2009). In particular, single-molecule fluorescence studies in vitro showed that the repetitive movement of the *E. coli* Rep translocase monomer on single-stranded DNA (ssDNA) can delay the formation of recombination intermediates (Myong et al., 2005), and in the case of PcrA helicase, this activity can lead to catalytic disruption of the recA-DNA filament (Park et al., 2010). Direct observation of repetitive helicase translocation on ssNA is a capability unique to single-molecule methods and highlights their power in mechanistic studies of nucleic acid translocases.

DNA Replication

In the decade that followed the now famous paper by Watson and Crick on the structure of DNA, Arthur Kornberg and his group, working with *E. coli* cell extracts, showed that the building blocks of the reaction were deoxynucleoside tri-phosphates (Bessman et al., 1958; Lehman et al., 1958), that these building blocks could yield a copy of the DNA molecule in a thermodynamically spontaneous reaction with a DNA template, and that this reaction, however energetically possible, required a catalyst to proceed at biologically compatible rates; they called the enzyme that they isolated "DNA polymerase" (Lehman et al., 1958) (now called DNA polymerase I). These enzymes are universally present across species (see Supplemental Information).

Many of these enzymes contain two active sites, a polymerization (pol) site that catalyzes the synthesis of dsDNA from an ssDNA template and an exonucleolysis (exo) site, capable of hydrolyzing and excising bases incorporated erroneously, greatly increasing the fidelity of the enzyme. DNA polymerases are distributive enzymes that require processivity factors to remain bound to the DNA template during replication. Thus, instead of tethering the enzyme and one end of the template,

as in transcription assays (see below), in single-molecule manipulation experiments one must tether both ends of the template. In the first study of this type, a single molecule of ssDNA was spanned between one bead held atop a micropipette by suction and another kept in an optical trap (Wuite et al., 2000). To follow the activity of T7 DNA polymerase, these authors took advantage of the difference in extension between ssDNA and dsDNA under all tensions (Box 2). As the enzyme converted ssDNA into dsDNA, the tweezers instrument, to keep the tension on the DNA constant at a preset value, changed the separation between the beads in an amount proportional to the progress of the enzyme. The authors observed bursts of polymerization activity, whose lengths were enzyme concentration and force independent, followed by gaps of constant extension whose lengths depended on enzyme concentration. These data indicated that each burst of activity corresponded to a different DNA polymerase binding, polymerizing, and falling off the template. It was estimated that the processivity of this polymerase is only around 420 bases (at 15 pN of tension). The rate of DNA polymerization decreased with increasing template tension until a (reversible) stall was reached at tensions around 34 pN. Surprisingly, the application of tension around and above this value induced exonucleolysis at rates 100 times faster than in solution. Based on these observations and analysis of the crystal structure of the ternary elongation complex (polymerase, incoming nucleotide, and DNA) (Doublie et al., 1998), the authors proposed a model in which two bases of ssDNA are organized within the enzyme during polymerization. Application of high forces deforms the DNA at the active site triggering the transfer of the 3′ end to the exonucleolysis site. Lowering the force below this threshold value allows the enzyme to resume polymerization.

Experiments with T7 DNA polymerase were complicated by the enzyme's low processivity: the observed kinetics of polymerization and exonucleolysis were convolved with the enzyme's on and off rates. Ibarra et al. (2009) studied the effect of force on the transfer dynamics between the pol and exo sites of φ29 DNA polymerase, an enzyme with a processivity greater than 70 kb. Again, this assay monitored the single-molecule conversion of ssDNA into dsDNA and vice versa by individual polymerases. Two mutants were studied besides the wild-type enzyme, an exo-deficient variant that lacks exo activity and a transfer-deficient mutant that cannot transfer the DNA between the pol and exo domains. Polymerization rate was found to be independent of force for a wide range of forces. However, above this range, polymerization speed decreased rapidly until all activity ceased at a force of ~37 pN for the wild-type enzyme. Upon lowering the tension, activity resumed, indicating that the stalling was reversible. Tensions above 46 pN or as low as 30 pN induced exonucleolysis activity in the presence (saturating conditions) or absence of dNTPs, respectively. Analysis of the enzyme's pausing and elongating behavior as a function of tension suggests that the tension mimics the presence of a nucleotide mismatch that distorts the DNA primer-template interactions triggering the exo editing response. This study revealed two intermediate states of the replication complex in the pol-exo transfer reaction. One of them appears to be a fidelity checkpoint before the pol-exo transfer.

Still, DNA replication in vivo is a more complex process because it involves both leading- and lagging-strand synthesis, as well as additional proteins that together form the replisome. Furthermore, due to the antiparallel nature of DNA strands and the 5′-3′ polarity of DNA polymerases, discontinuous pieces of DNA, known as Okazaki fragments, must be synthesized on the lagging strand (Ogawa and Okazaki, 1980). In order to coordinate the synthesis of the Okazaki fragments with the leading-strand polymerase, a DNA loop is thought to be formed between the leading polymerase at the replication fork and the polymerization site on the lagging strand (Alberts et al., 1983). Hamdan et al. (2009) have used a single-molecule technique to monitor the formation and release of these loops for single bacteriophage T7 replisomes. Four proteins form the T7 replisome, one of the simplest known: the polymerase, the helicase-primase protein gp4, the gp5-thioredoxin protein clamp, and the gp2.5 single-stranded binding protein. In this single-molecule experiment, the lagging strand of a DNA replication fork was attached to a glass slide while the downstream DNA was attached to a bead and kept under force (see Figure S2). In the presence of all four proteins as well as a full set of deoxynucleotides and the ribonucleotides required for primer synthesis, a shortening followed by a lengthening of the DNA was observed, presumably corresponding to the formation and release of the loop.

Two models have been proposed for the triggering of loop release: the signaling and collision models. In the signaling model, primase activity is responsible for the timing of loop release, independently of the completion of the Okazaki fragment. In contrast, the collision model proposes that the arrival of DNA polymerase to the end of the previous Okazaki fragment causes loop release. For this model, however, leading-strand polymerization must continue even after loop release to allow the primase to find its next starting sequence. This additional polymerization length would then increase the size of the next loop formed, a directly testable prediction. Indeed, analyses of the data show a positive correlation of the lag time between the formation of two loops and the loop length, consistent with the collision model. However, by changing the concentration of the available ribonucleotides for primer synthesis or by substituting them with dinucleotides, a change in both the length of the loop and the lag time between loops was observed. These data then indicated that the first step in RNA primer synthesis—the formation of the first two RNA bases—triggered loop release and argued instead for the signaling model. The authors concluded that not being mutually exclusive, both mechanisms operate during DNA replication.

Additionally, using single-molecule fluorescence resonance energy transfer (FRET), researchers have begun to understand other specialized types of DNA polymerases, such as the HIV reverse transcriptase (Liu et al., 2008) and telomerase (Wu et al., 2010) (see Supplemental Information). Even though some progress has been made, there is still a long way before the complex dynamics of these enzymes are fully revealed.

DNA Transcription

RNA polymerase is the enzyme responsible for the first step of gene expression: copying the information stored in DNA into the messenger RNA (mRNA). The prokaryotic RNA polymerase,

RNAP, is a 450 kDa protein with five core subunits and one initiation factor. Of the various RNA polymerases that exist in eukaryotes, RNA polymerase II (Pol II)—the one responsible for the synthesis of mRNA, some small nuclear RNAs (sNRNA), and most microRNAs—is the most studied. Pol II has a molecular weight close to that of its prokaryotic counterpart (550 kDa), it is composed of 12 subunits, and it requires a rather large number of factors to initiate transcription. For both enzymes, the transcription cycle consists of three stages: initiation, elongation, and termination. During initiation, the polymerase, with the help of initiation factors, binds to the promoter sequence in the template DNA and unwinds the duplex, forming a transcription bubble in an open promoter complex (OPC). The polymerase then undergoes a series of attempts known as abortive initiation in which short pieces of RNA are formed but detach from the complex. It is not until the growing RNA reaches a length of around 9–11 bases that the complex makes the transition into the elongation stage. As part of elongation and as it reads the template DNA in the 3′ to 5′ direction, RNAP displaces the transcription bubble base by base, opening the next base pair in front and closing a base pair at its back. At each DNA base, RNAP binds the next correct ribonucleoside tri-phosphate (NTP), hydrolyzes it, incorporates it into the 3′ end of the RNA growing chain, and releases pyrophosphate (PPi). During termination, the enzyme reads the terminator sequence and detaches from the DNA, releasing the transcript. Termination can occur either in a Rho-independent or in a Rho-dependent manner. In the former, a very stable RNA hairpin and a U-rich track are required to destabilize the complex. In the latter, Rho, an RNA helicase, moves along the transcript until it reaches the enzyme and releases the transcript.

RNA polymerase has been studied by means of an ever-growing array of techniques. Traditional biochemical bulk methods, together with recent structural breakthroughs, have set the stage for much of what is known about this molecular motor. However, these approaches cannot provide a detailed picture of the dynamics of transcription, as much of the details of the individual molecular trajectories are lost in the asynchronous average of the signals. In contrast, single-molecule methods have made it possible to follow the individual transcription traces, characterize their heterogeneity, and reveal their stochastic alternation in periods of continuous translocation and pauses.

Initiation Studies

Initiation is the process by which RNA polymerase binds to a promoter sequence and locally unwinds the DNA template to form the OPC. Atomic force microscopy (AFM) studies have revealed that λ_{PR} promoter wraps around the polymerase over 270° in OPCs and that 2/3 of this wrapping involves extensive contacts of the enzyme with the upstream DNA (Rivetti et al., 1999). At this point, the catalytic center of the polymerase will be located at the +1 site of the template from which RNA synthesis will start. Most single-molecule studies of initiation have been performed on prokaryotic RNA polymerase due to the vast complexity of eukaryotic initiation. In bacteria, only one transcription factor is required for initiation, the sigma factor. In *E. coli* sigma-70 is the housekeeping factor, but other factors, like sigma-32, the heat shock sigma factor, also exist.

In recent years, single-molecule fluorescence has risen as a powerful tool for analyzing the dynamics of initiation. Kapanidis et al. (2005) used FRET to render the first quantitative study of the extent of sigma-70 retention during the transition from initiation to elongation. The authors placed a donor-acceptor pair on the sigma subunit of the polymerase and on either the downstream or upstream template DNA. By measuring changes in FRET efficiency they were able to assess both the translocation state of the polymerase and the presence or absence of the sigma factor as a function of transcript length. Contrary to previous biochemical results that argued sigma-70 detachment upon the transition from initiation to elongation, this single-molecule experiment proved that, for the lacUV5 promoter, the sigma factor is retained for approximately half of the transcription elongation complexes, even for mature elongation complexes with 50 bp transcripts. Margeat et al. (2006) performed a similar experiment but with surface-immobilized complexes and not only again confirmed sigma-70 retention by elongation complexes but, more importantly, conclusively eliminated the possibility of sigma factor rebinding, a plausible concern for solution experiments. Together, these experiments convincingly demonstrate that sigma release is not required for promoter escape and challenge the conventional belief of sigma disengagement as part of the transition between initiation and elongation. However, as Kapanidis et al. point out, sigma retention in vivo could be different due to the presence of other transcription factors that might facilitate sigma release.

Three different movement mechanisms involved in the early dynamics of transcription initiation have been proposed: inchworming, scrunching, and transient excursions (Kapanidis et al., 2006; Revyakin et al., 2006; and references therein). In the inchworming model, a portion of the polymerase containing its catalytic center and the complete transcription bubble moves forward on the DNA, while its trailing edge remains static. This mechanism requires that the polymerase be somewhat elastic, extending and contracting as it moves along DNA. The scrunching hypothesis postulates that the polymerase remains static with respect to the DNA, but that it reels in the template keeping the extra DNA inside. Finally, the transient excursion model proposes that the entire polymerase moves rapidly forward and backward along the DNA as it creates abortive products. Two separate studies, using two distinct single-molecule methods, have evaluated the predictions of these three models. Revyakin et al. (2006) used a magnetic tweezers assay in which changes in extension of supercoiled DNA are observed upon unwinding due to initiation. Their results show an initial unwinding due to DNA bubble opening as expected but, surprisingly, also an additional unwinding whose extent depends on the length of the abortive RNA product. Only the scrunching model predicts increased unwinding during abortive initiation because the reeled-in DNA bases are unwound and kept as single-stranded bulges inside the polymerase. The two other mechanisms should only advance the transcription bubble but not change the unwound state of the DNA. Based on these results the authors conclude that all transcription complexes undergo scrunching during initiation for transcripts longer than 2 bp and propose that it is precisely the creation of this stressed intermediate that facilitates promoter escape. Along the same lines, Kapanidis et al. (2006) have used

a single-molecule FRET experiment to test these three models. Donor-acceptor pairs in specific locations on the initiation complex are used as reporters of changes in distance. With this method the authors find that during abortive initiation, there is a change in extension between the leading edge of the polymerase and the downstream end of the DNA, as expected, but not a measurable distance change between the trailing edge of the polymerase and the upstream DNA (eliminating the transient excursion model) or between two positions on the enzyme (invalidating the inchworming model). These results, again, independently support the DNA scrunching mechanism.

The observation of partial loss of upstream contacts during abortive transcription of a 6-mer and 8-mer (Straney and Crothers, 1987) suggests that abortive initiation may result from the failure of the enzyme to fully break these contacts. The energy required to break the association of the enzyme to the promoter has been estimated in roughly 10–15 kcal/mol (Murakami et al., 2002). On the other hand, the maximum work that the prokaryotic enzyme can generate is roughly ~0.8–1 kcal/mol using one-half of 0.34 nm per base pair for the distance to the transition state and between 20–25 pN for the stall force of the motor (see below). Therefore, the motor cannot climb the required energetic hill in a single step. More likely, the enzyme "peels" itself off from the promoter through successive catalytic cycles during abortive initiation, breaking partial interactions with the promoter one step at a time. It was early suggested that some kind of stress intermediate could be responsible for the escape and clearance of the promoter (Straney and Crothers, 1987). The finding of DNA scrunching provides a candidate for that intermediate and a mechanism for the storage and accumulation of at least part of the work done by the enzyme during its separation from the promoter. This stored energy should increase as the DNA is compressed inside the enzyme until the scrunched DNA is released either at the front of the polymerase (abortion followed by release of the short transcript) or at its back (formation of stable elongation complex).

Elongation and Pausing

The first study of RNAP's ability to move against an external opposing force and generate work was done by Yin et al. (Yin et al., 1995) using optical tweezers. By immobilizing an *E. coli* RNA polymerase molecule on a glass slide and attaching a polystyrene bead to the downstream end of the DNA, they observed individual transcription events under force. These authors determined that *E. coli's* enzyme generates average forces as high as 14 pN before stalling. Later experiments (Wang et al., 1998) yielded mean stall forces of 25 pN, a value more than five times those of myosin and kinesin but small compared to forces exerted by other DNA translocases (Chemla et al., 2005), as described before.

Analysis of the RNAP's force-velocity behavior (Wang et al., 1998) revealed that the translocation velocity of the enzyme is largely unaffected by the force until the maximum force is reached, and that, at the single-molecule level, transcription was made up of alternating continuous translocation and stochastic pausing events. A more systematic study of the kinetics of the enzyme's pausing behavior (Davenport et al., 2000) demonstrated that translocation and pausing compete kinetically, suggesting that pauses states are off the main elongation pathway. This study also revealed that the paused state is an intermediary to irreversible motor arrest. Forde et al. (2002) studied the effect of opposing and assisting force and of nucleotide concentration on elongation velocity and pause entry. Their data show that lower nucleotide concentrations lead to decreased velocity and increased pausing, again confirming the kinetic competition between the main elongation pathway and the off-pathway paused state.

As the resolution and precision of optical tweezers experiments improved, more detailed studies of RNAP pausing became possible. Shaevitz et al. (2003) observed backward movements along the DNA and identified them with the backtracking events described by bulk studies when the polymerase was shown to move backward displacing the 3′ end of the transcript from its catalytic center (Nudler et al., 1997). In parallel, Neuman et al. described short polymerase pauses that could be well fit by a double exponential and were force independent, arguing against a backtracking mechanism (Neuman et al., 2003). Therefore, these two studies claimed the existence of two distinct types of pauses: "ubiquitous" pausing in which backtracking does not occur, and backtracked pauses. Another study (Dalal et al., 2006) analyzed the effect of RNA secondary structure on ubiquitous pauses by pulling on the 5′ end of the nascent RNA during transcription. They did not observe a significant effect on the enzyme's processivity, elongation rate, pause frequency, or pause lifetimes, thereby concluding that ubiquitous pauses are not related to the formation of RNA hairpins. In addition, Herbert et al. (2006) studied the sequence dependence of pausing and proposed that ubiquitous pauses are associated with DNA sequences similar to known regulatory pause sequences.

This conclusion was challenged when Galburt et al. (2007) demonstrated that pause durations for the yeast polymerase (Pol II) follow a power-law distribution of $t^{-3/2}$. These authors proposed that such dependence arises naturally if, during backtracking, the transcription bubble moves backward and forward executing an isoenergetic one-dimensional diffusion along the DNA. A pause ends when the 3′ end of the RNA realigns at the active site so that elongation can resume. These distributions suggested that most if not all pauses observed are backtracking pauses. This same mechanism for pausing was later verified for the *E. coli* polymerase as well (Mejia et al., 2008).

The earlier observation that some pauses do not appear to involve backtracks was recently addressed by Depken et al. (2009). In this work, backtracking was modeled as a discrete one-dimensional random walk, with an absorbing boundary, along the periodic potential of the DNA. The distribution derived from their model predicts three regimes as a function of pause duration. Short pauses have a probability density that falls off exponentially, whereas intermediate pause durations follow a $t^{-3/2}$ decay that is then cut off by an exponential behavior for even longer pause durations. Furthermore, they also showed that the pauses within the short time limit would display apparent force insensitivity, and very brief and shallow backward excursions, both characteristics observed for the ubiquitous pauses. Therefore, these authors conclude that a single mechanism, backtracking, can account for the behavior of most if not all pauses observed.

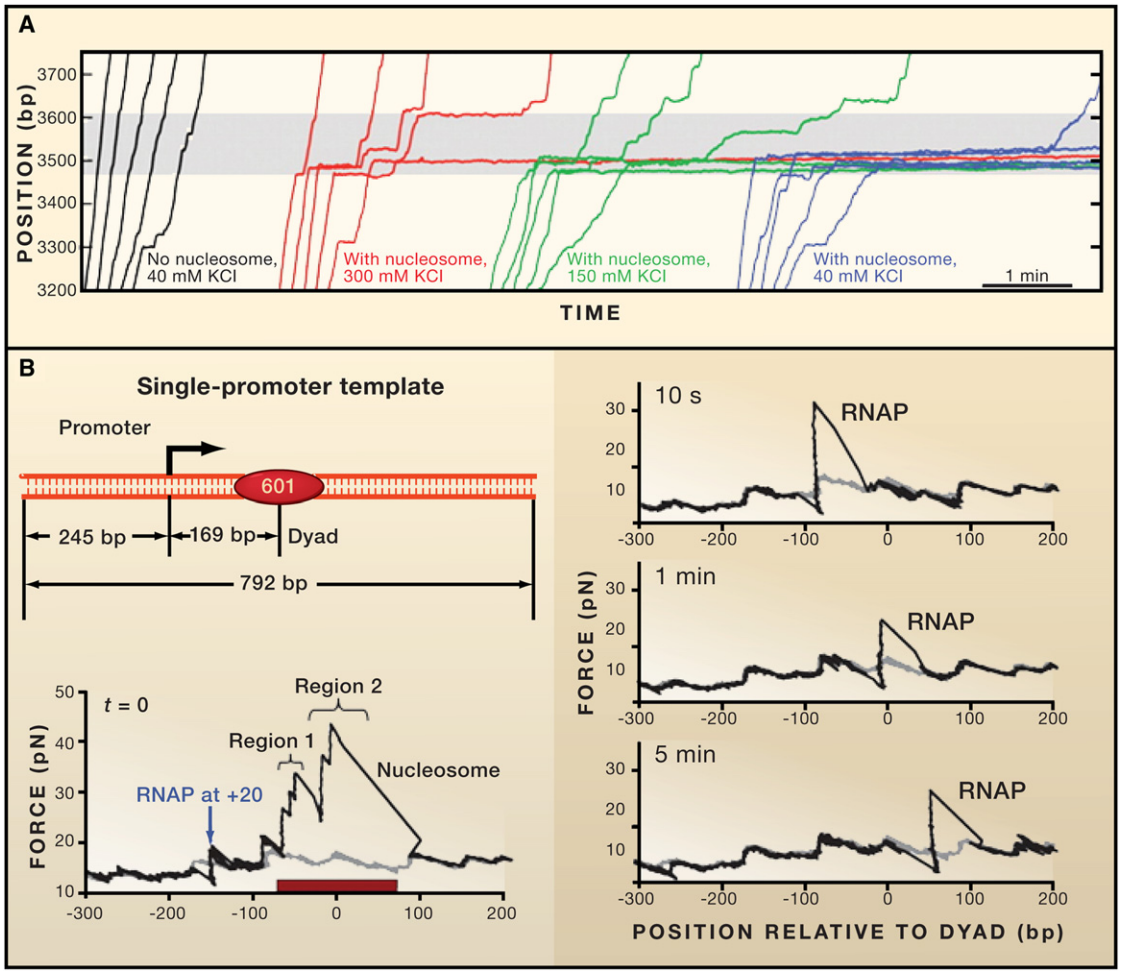

Figure 3. Transcription through the Nucleosome

(A) Hodges and Bintu (Hodges et al., 2009) follow Pol II transcription through the nucleosome in real-time. They observe an increase in the probability of nucleosome passage with ionic strength, as well as an increase in pause density and pause duration in the vicinity of the nucleosome. Their model supports a passive mechanism of motion that depends on thermal fluctuations of the DNA-nucleosome interactions.

(B) Jin et al. (2010) use an unzipping technique to infer the position of the polymerase after transcription has occurred. They also observe increased pausing within the nucleosomal sequence and verify nucleosome-induced polymerase backtracking of 10–15 bp. The inclusion of RNase or a trailing polymerase limits backtracking and increases the passage probability (adapted from Hodges and Bintu et al. [Hodges et al., 2009] and Jin et al. [2010]).

Surprisingly, the first studies of Pol II revealed that it stalls at an opposing force two to three times smaller (~7 pN) than its prokaryotic counterpart due to its greater tendency to enter a backtrack (Galburt et al., 2007). This was a surprising finding, given that the natural substrate for this enzyme is not bare but nucleosomal DNA. These authors also found that addition in *trans* of TFIIS, a transcription factor known to activate cleavage of the 3′ end of the transcript by backtracked Pol II complexes, increases the stall force of the enzyme by 3-fold. They proposed that the weaker mechanical performance of RNAP is part of a regulatory mechanism of transcription elongation in eukaryotes.

Transcription through the Nucleosome

How does RNA polymerase overcome hurdles along the transcriptional path? What is the physical basis underlying the regulation of eukaryotic gene expression by nucleosomal DNA? Hodges and Bintu (Hodges et al., 2009) used an optical tweezers instrument to observe Pol II transcription of a template containing a single nucleosomal particle. Their data show that the probability of transcribing over the nucleosomal barrier increases sharply with the ionic strength of the environment (Figure 3), presumably due to the decreased stability of the nucleosome-DNA interactions under high screening conditions. The presence of the nucleosome increased the local pause density (as compared to that of bare DNA), slowed pause recovery (increased pause duration), and slightly reduced elongation speed. Interestingly, their data indicate that during transcription the polymerase does not actively separate the DNA from the nucleosome. Instead, it waits for thermal fluctuations that cause local unwrapping of the nucleosomal DNA in order to advance. Thus, the polymerase acts as a rectifier of nucleosome fluctuations, consistent with the ratchet mechanism of motion

proposed for the operation of RNAP (Bar-Nahum et al., 2005). Based on these results, they developed a quantitative model in which the nucleosome behaves as a *fluctuating* mechanical barrier that slows forward translocation and causes the polymerase to enter backtracked/paused states and, as a result, increases the probability of enzyme arrest. Furthermore, during backtracks the nucleosome can rewrap the newly exposed DNA, a process that slows down the recovery from a pause.

As a way to better understand the interactions between the DNA and the nucleosome, Jin et al. (2010) developed a DNA unzipping technique that monitors the position of RNA polymerase from *E. coli* on the DNA template after transcription (Figure 3B). In this experiment, a nucleosome is placed downstream of a polymerase and, after transcription is allowed to take place for varying periods of time, the two strands of the transcribed molecule are pulled apart. The bacterial polymerase does not encounter nucleosomes in vivo, however it is used as a model system warranted by the high level of functional homology with Pol II (Walter et al., 2003). The resulting force extension curves show characteristic transitions that indicate the position of the polymerase on the DNA (to avoid additional transitions due to nucleosome unwrapping, the nucleosome was removed from the template using heparin). The authors observed nucleosome-induced polymerase pausing with a 10 bp periodicity that was sequence independent and correlated with the periodicity of the interactions between the nucleosome and the DNA. Moreover, by comparing the size of the RNA formed (using a transcription gel) with the position of the polymerase on the template (using the unzipping assay), they estimated that the polymerase backtracks between 10–15 bases when it encounters the nucleosome. They further reasoned that, if backtracking and arrest occur upon transcription through the nucleosome, conditions under which backtracking is limited should facilitate passage. As predicted, the use of RNase, as a way to reduce the number of RNA bases the polymerase could backtrack on, decreased the number of backtracked bases and increased the number of complexes that passed the nucleosome. Similarly, the addition of a second trailing polymerase that physically limited the number of bases the leading polymerase could move back enhanced passage by a factor of 5, an amount similar to experiments using RNase. From these experiments the authors speculate that the presence of multiple polymerases in vivo will further facilitate transcription through the nucleosome by preventing or reducing backtracking. Also, transcription factors like TFIIS could rescue backtracked polymerases, expediting nucleosome passage. It would be interesting to repeat these experiments with the eukaryotic enzyme.

RNA polymerase pausing and backtracking are intrinsic and complex properties of RNA polymerase important for transcription regulation and control of transcription fidelity. Future use of mutant polymerases with altered pausing behavior and the reconstitution in vitro of ever more complex single-molecule transcription reactions should provide a more complete picture of the mechanisms that control gene expression during transcription elongation.

Transcription Termination

To investigate the importance of mechanical force on termination, forces up to 30 pN were applied to the nascent RNA transcript (Dalal et al., 2006). No significant effect was found on enzyme processivity, elongation rates, pause frequencies, and lifetimes. It is unlikely that the termination hairpin or Rho could exert larger forces; thus if force plays any role in termination, it must be aided by an allosteric effect wherein the binding energy of the hairpin and/or Rho to the complex pay in part the energetic price of disrupting the DNA-RNA hybrid. Larson et al. (2008) found that pulling between RNAP and upstream DNA does not affect termination efficiency on two out of three terminators studied, indicating that hypertranslocation (forward movement of the bubble with respect to RNA's 3′ end) either cannot be effected mechanically or is not the only mechanism of termination. In fact, the authors propose that depending on the identity of the terminator, shearing of the RNA-DNA hybrid or hypertranslocation, or both, can occur during transcript release.

Prokaryotic Translation

Ribosomes are the cellular machines that hydrolyze GTP to "read" and translate the information encoded in mRNA into protein (Moore and Steitz, 2003). Single-molecule studies of translation are quite recent and restricted to prokaryotic ribosomes. Translation is an extremely complex process also conveniently divided in three phases: initiation, elongation, and termination (Ramakrishnan, 2002).

In prokaryotes, initiation begins with the binding of the ribosome to the methionine-encoding mRNA translation start codon, AUG, whose placing at the P site of the ribosome is directed by an upstream Shine-Dalgarno (SD) sequence complementary to a segment of the 16S ribosomal RNA. Initiation requires initiation factors IF1, IF2•GTP, and IF3.

In elongation, ternary complexes of tRNAs charged with the correct amino acids, elongation factor EF-Tu, and GTP bind to ribosome. The correct amino acid-carrying tRNA is selected by its complementarity to the codon on the mRNA and interactions with the small and large subunits at the A site of the ribosome. Upon GTP hydrolysis and release of EF-Tu, the tRNA is bound in the "classical" position at the A site, adjacent to the peptide-containing tRNA bound in the classical position at the P site. Subsequently, a new peptide bond is formed as the polypeptide in the P site is transferred to the A site tRNA, a reaction catalyzed by the peptidyl transferase active site in the 23S rRNA of the 50S subunit. This event allows the tRNAs to access intermediate binding conformations called "hybrid" states, in which the anticodon ends of the tRNAs remain in their classical A and P sites in the 30S subunit but their acceptor stems make contacts in the P and E sites of the 50S subunit, respectively (Moore and Steitz, 2003). The elongation cycle is completed with the translocation of the ribosome relative to the mRNA upon binding of another elongation factor, EF-G•GTP, and the subsequent hydrolysis of GTP. In this process, the tRNA at the A site moves to the P site and the tRNA at the P site moves to the exit or E site.

Termination occurs when the ribosome encounters a stop codon (either UAA, UAG, or UGA). Protein release factors are bound that cleave the peptide from the tRNA at the P site; release factor 1 (RF1) recognizes UAA and UAG; release factor 2 (RF2) recognizes UAA and UGA. The ribosome then remains attached to the mRNA. Dissociation of the ribosome into its

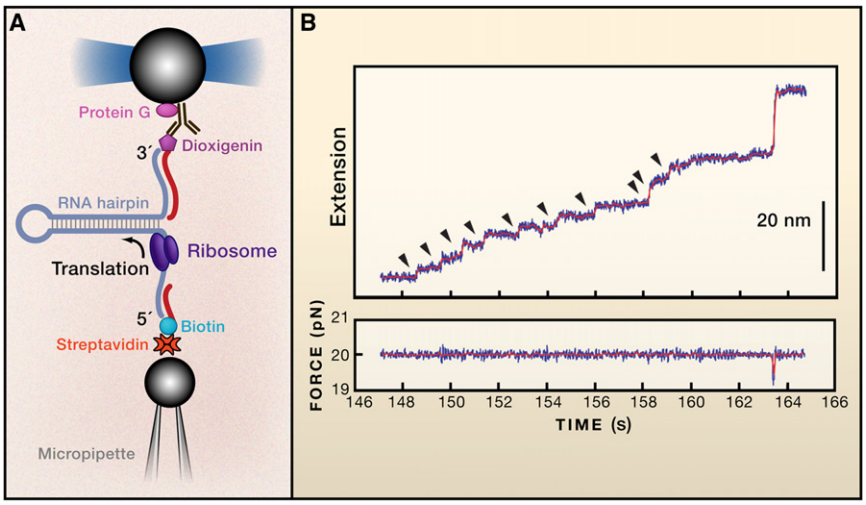

Figure 4. Single-Molecule Studies of Ribosomes

(A) Experimental design for monitoring single ribosome translation in real-time. The ribosome was stalled at the 5′ side of the mRNA hairpin construct, which was then held between two polystyrene beads. Drawings are schematic and not to scale.

(B) Single ribosome trajectory through an mRNA hairpin as in (A). Data obtained at constant force (lower panel). The arrows represent individual codon steps (Wen et al., 2008).

component subunits requires ribosome-recycling factor, RRF (Liljas, 2004), and EF-G.

Optical tweezers have been used to pull the mRNA from the ribosome in various conditions (Uemura et al., 2007). The strength of the ribosome-mRNA interactions increased by ~5 pN when deacylated $tRNA^{fMet}$ was bound to the P site. A $PhetRNA^{Phe}$ at the A site stabilized the P-site-bound ribosome by ~10 pN. A SD sequence further strengthened the interaction by ~10 pN. A peptidyl-tRNA analog N-acetyl-Phe-$tRNA^{Phe}$ bound to the A site weakened the rupture force in an SD-independent manner relative to the complex carrying a Phe-$tRNA^{Phe}$, indicating that following peptide bond formation, the ribosome looses grip of the mRNA to complete translocation.

Recently, optical tweezers were used (Wen et al., 2008) to monitor translation of an RNA hairpin by single *E. coli* ribosomes using a helicase-based assay (see Figure 4A) similar to the one used previously for the studies of NS3 helicase (see above). Ribosomes load at a start side on the 5′ side of the hairpin. At the beginning of the experiment, a preset force is applied to the ends of the hairpin and held constant via a feedback circuit in the instrument. As the ribosome translates each codon in the hairpin, six bases are converted into ssRNA, making the molecule longer and requiring the beads to be moved apart to keep the force constant. At 20 pN, each codon corresponds to a bead displacement of 2.7 nm. These studies have revealed that translation occurs through successive translocation-and-pause cycles (see Figure 4B). The distribution of pause lengths, with a median of 2.8 s, reveals that at least two rate-determining processes control each pause. Each translocation step occurs in less than 0.1 s and measures three bases—one codon—indicating that translocation and RNA unwinding (helicase activity) are strictly coupled ribosomal functions. Pause lengths, and therefore the overall translation rate, depend on the secondary structure of the mRNA. Unlike in the case of the NS3 helicase (see above), the external force applied to the hairpin reduces the magnitude of the kinetic barrier at the junction and decreases pause durations. It does not, however, affect the actual translocation times.

Although single-molecule manipulation studies of translating ribosomes have just started, these codon-resolution experiments should provide answers to questions such as: Does the codon sequence affect the dwell time of the ribosome at a pause? Is the ribosome a passive or an active helicase? How are the single ribosome helicase trajectories affected by the concentration of EF-G and EF-Tu? How does the ribosome respond in real-time to barriers such as hairpins, pseudo-knots, and other structures? How powerful is the ribosome as a motor? That is, what kind of forces can it develop? How does the ribosome translation rate respond to direct mechanical load, or in other words, what is the ribosome velocity versus force curve? What is the distance to the transition state for translocation? How do frameshifts occur and what are their microscopic dynamics? Finally, by directly grabbing the nascent polypeptide, it will be possible to follow in real-time its folding dynamics on the surface of the ribosome.

Single-molecule FRET has been used also to explore translation. Fluorescently labeled phe-tRNAs have been used to reveal tRNA dynamics during elongation (Blanchard et al., 2004a, 2004b; Lee et al., 2007; Marshall et al., 2008). Cy5-labeled Phe-$tRNA^{Phe}$ ternary complexes delivered to 70S elongation complexes bound to Cy3-labeled fMet-$tRNA^{fMet}$. tRNAs were seen to attain a high-FRET state from low- and middle-FRET states in about 100 ms. The low-FRET state was shown to correspond to the initial selection of the tRNA at the A site, the middle-FRET state to correspond to the GTPase activation ensuing the binding of the cognate tRNA, and the high-FRET state to correspond to the full tRNA accommodation. These single-molecule experiments revealed that binding of the ternary complex to the ribosome is made up of two components: a codon-independent binding of the complex to L7/L12 proteins with zero FRET and a codon-dependent, reversible, rapid (50 ms) sampling of the A-site codon leading to the low-FRET state. Following accommodation and formation of the high-FRET state, a reversible transition to a second mid-FRET state was observed (Blanchard et al., 2004b), which was identified as the signature of the hybrid state.

Single-molecule FRET has also been used to investigate the dynamics of the internal degrees of freedom of the ribosome. During translocation, the large and the small subunits are known to rotate by 10° relative to each other (Frank et al., 2007).

This "ratchet" motion is thought to accompany the formation of the hybrid states (Ermolenko et al., 2007). Fluctuations in the spatial orientations of the large and small subunits were followed in real-time by FRET changes between Cy3-labeled protein L9 and Cy5-labeled protein S6 (Cornish et al., 2008). Ribosomes fluorescently labeled at L1 and L33 were also used to monitor the movement of the L1 stalk of the E site (Cornish et al., 2009). A correlation between the L1 stalk position and the binding, movement, and release of the deacylated tRNA at the E site was found, suggesting that conformational changes of the stalk are responsible for the tRNA transitions. Consistent with these observations, fluctuating FRET signals between the L1 stalk and the incoming tRNA were also detected (Fei et al., 2008). These signals were thought to represent the stochastic movements of the L1 stalk between open and closed conformations in the pretranslocation elongation complex, coupled to the fluctuations of the P-site tRNA between its classical and its hybrid configurations. Taken all together, these observations suggest that the deacylation of the peptidyl-tRNA during elongation triggers the fluctuation of the entire pretranslocation complex between two major conformational states, global state 1 (GS1) and global state 2 (GS2) (Fei et al., 2008). Evidence for these two global states has been recently found by two Cryo-EM studies (Agirrezabala et al., 2008; Julian et al., 2008).

Single-molecule FRET has been used to investigate the dynamics of the ribosome and tRNAs during translation termination and ribosome recycling (Sternberg et al., 2009). These authors used fluorescently labeled RF1, tRNAs, and ribosomes to show that when RF1 binds at a stop codon and promotes the hydrolysis of the peptide, the ribosome is locked in the GS1 state. Subsequent binding of RF3 and GTP induce the ribosome to transition into GS2 and RF1 to release. GTP hydrolysis then ensues and primes the ribosome for recycling. The authors showed that the effect of RRF is to bias the state of the ribosome to GS2, the recycling-competent state.

The implementation of single-molecule approaches together with new technical developments such as zero-mode waveguides (ZMWs) allowed Uemura et al. (2010) to follow in real-time the binding of tRNA during processive translation at physiologically relevant micromolar ligand concentrations. By labeling the tRNAs with distinct fluorophores, these authors were able to determine the identity of the tRNA and the mRNA codon involved. This study found that ribosomes are only briefly occupied by two tRNA molecules and that release of deacylated tRNA from the exit (E) site is uncoupled from binding of aminoacyl-tRNA site (A site) tRNA, occurring rapidly after translocation.

Perspective

The minimal unit of living matter, the cell, is a complex microscopic factory whose integrity and homeostasis depend on the operation of an interconnected network of highly specialized tiny processing units or molecular machines. Some of these machines, like the ones that are the subject of this Review, must function as nucleic acid translocases. They must move along their nucleic acid templates to read, copy, and translate the linear information encoded in their sequences and ensure the flow, control, and expression of genetic information. Until recently, the detailed study of their function had lagged behind that of their structures, mainly because of the difficulty of synchronizing a population of molecules to follow their dynamics. This situation is now changing rapidly. The emergence over the last two decades of single-molecule techniques has begun to yield impressive details on how these macromolecular machines work. By following the actual molecular trajectories of these translocases, and not just the mean or average behavior of a population of molecules, we are beginning to learn unprecedented details of their complex dynamics, the manner by which they move on nucleic acids, the mechanical nature of their moving parts, the presence of transient intermediates, their mechanisms of fidelity, and the manner in which they use the spontaneous fluctuations of the bath to accomplish their mechanical tasks.

We have many reasons to believe that these developments are just the beginning of growing insight into the operation of these machines: with the advent of high-resolution, single-molecule optical tweezers (Abbondanzieri et al., 2005; Moffitt et al., 2006) and the combination of optical tweezers with single-molecule fluorescence capability (Hohng et al., 2007; Lang et al., 2004), it should be possible now to monitor directly the movement of motors at angstrom-level resolution (Moffitt et al., 2009) and to uncover the coordination of their various parts during their mechanochemical conversion (Ishijima et al., 1998).

Future efforts, through the study of ever more complex assemblies, will also likely try to fill the gap between the controlled experimental conditions of in vitro studies and the need to understand at a quantitative level how the performance of these machines is influenced by their physiological partners (Stano et al., 2005). Finally, recent advances in super-resolution optical imaging (Betzig et al., 2006; Hell, 2007; Huang et al., 2008) may also make it possible to fulfill the ultimate hope of directly observing the activity of these machines in living cells.

Ultimately, a comparison of the diverse molecular designs utilized by evolution to accomplish these directional and energy-driven tasks, the unraveling of the physical principles that lie behind their function, and the emerging understanding of the importance of fluctuations in their operation and thermodynamic efficiency should provide, in the not-too-distant future, the basis for the development of a comprehensive theory of molecular motors. At the very least, we hope that these efforts will fulfill the goal of endowing the detailed structures of these molecular entities, with an equally detailed description of the molecular choreography that underlies their operation in the cell.

SUPPLEMENTAL INFORMATION

Supplemental Information includes an Extended Discussion, two figures, and Supplemental References and can be found with this article online at doi:10.1016/j.cell.2011.01.033.

ACKNOWLEDGMENTS

We thank Timothy M. Lohman at Washington University School of Medicine for a critical reading of the draft on helicases and many colleagues for stimulating discussions. The literature on nucleic acid translocases, in particular their single-molecule studies, is ever increasing. Due to space limitations and our coverage of selected topics, we would like to apologize to our colleagues who actively work on nucleic acid translocases yet whose work has not been cited here. C.B. was supported by NIH, DOE, and HHMI. W.C. was supported by Ara Paul Professorship fund at the University of Michigan Ann Arbor.

REFERENCES

Aathavan, K., Politzer, A.T., Kaplan, A., Moffitt, J.R., Chemla, Y.R., Grimes, S., Jardine, P.J., Anderson, D.L., and Bustamante, C. (2009). Substrate interactions and promiscuity in a viral DNA packaging motor. Nature *461*, 669–673.

Abbondanzieri, E.A., Greenleaf, W.J., Shaevitz, J.W., Landick, R., and Block, S.M. (2005). Direct observation of base-pair stepping by RNA polymerase. Nature *438*, 460–465.

Aboussekhra, A., Chanet, R., Adjiri, A., and Fabre, F. (1992). Semidominant suppressors of Srs2 helicase mutations of Saccharomyces cerevisiae map in the RAD51 gene, whose sequence predicts a protein with similarities to procaryotic RecA proteins. Mol. Cell. Biol. *12*, 3224–3234.

Agirrezabala, X., Lei, J., Brunelle, J.L., Ortiz-Meoz, R.F., Green, R., and Frank, J. (2008). Visualization of the hybrid state of tRNA binding promoted by spontaneous ratcheting of the ribosome. Mol. Cell *32*, 190–197.

Ahnert, P., Picha, K.M., and Patel, S.S. (2000). A ring-opening mechanism for DNA binding in the central channel of the T7 helicase-primase protein. EMBO J. *19*, 3418–3427.

Alberts, B. (1998). The cell as a collection of protein machines: Preparing the next generation of molecular biologists. Cell *92*, 291–294.

Alberts, B.M., Barry, J., Bedinger, P., Formosa, T., Jongeneel, C.V., and Kreuzer, K.N. (1983). Studies on DNA replication in the bacteriophage T4 in vitro system. Cold Spring Harb. Symp. Quant. Biol. *47*, 655–668.

Antony, E., Tomko, E.J., Xiao, Q., Krejci, L., Lohman, T.M., and Ellenberger, T. (2009). Srs2 disassembles Rad51 filaments by a protein-protein interaction triggering ATP turnover and dissociation of Rad51 from DNA. Mol. Cell *35*, 105–115.

Appleby, T.C., Anderson, R., Fedorova, O., Pyle, A.M., Wang, R., Liu, X., Brendza, K.M., and Somoza, J.R. (2010). Visualizing ATP-dependent RNA translocation by the NS3 helicase from HCV. J. Mol. Biol. *405*, 1139–1153.

Bar-Nahum, G., Epshtein, V., Ruckenstein, A.E., Rafikov, R., Mustaev, A., and Nudler, E. (2005). A ratchet mechanism of transcription elongation and its control. Cell *120*, 183–193.

Bessman, M.J., Lehman, I.R., Simms, E.S., and Kornberg, A. (1958). Enzymatic synthesis of deoxyribonucleic acid. II. General properties of the reaction. J. Biol. Chem. *233*, 171–177.

Betterton, M.D., and Julicher, F. (2005). Opening of nucleic-acid double strands by helicases: active versus passive opening. Phys. Rev. E Stat. Nonlin. Soft Matter Phys. *71*, 011904.

Betzig, E., Patterson, G.H., Sougrat, R., Lindwasser, O.W., Olenych, S., Bonifacino, J.S., Davidson, M.W., Lippincott-Schwartz, J., and Hess, H.F. (2006). Imaging intracellular fluorescent proteins at nanometer resolution. Science *313*, 1642–1645.

Bianco, P.R., Brewer, L.R., Corzett, M., Balhorn, R., Yeh, Y., Kowalczykowski, S.C., and Baskin, R.J. (2001). Processive translocation and DNA unwinding by individual RecBCD enzyme molecules. Nature *409*, 374–378.

Bird, L.E., Subramanya, H.S., and Wigley, D.B. (1998). Helicases: a unifying structural theme? Curr. Opin. Struct. Biol. *8*, 14–18.

Blanchard, S.C., Gonzalez, R.L., Kim, H.D., Chu, S., and Puglisi, J.D. (2004a). tRNA selection and kinetic proofreading in translation. Nat. Struct. Mol. Biol. *11*, 1008–1014.

Blanchard, S.C., Kim, H.D., Gonzalez, R.L., Jr., Puglisi, J.D., and Chu, S. (2004b). tRNA dynamics on the ribosome during translation. Proc. Natl. Acad. Sci. USA *101*, 12893–12898.

Bryant, Z., Stone, M.D., Gore, J., Smith, S.B., Cozzarelli, N.R., and Bustamante, C. (2003). Structural transitions and elasticity from torque measurements on DNA. Nature *424*, 338–341.

Burroughs, A.M., Iyer, L.M., and Aravind, L. (2007). Comparative genomics and evolutionary trajectories of viral ATP dependent DNA-packaging systems. In Gene and Protein Evolution, J.-N. Volff , ed., pp. 48–65.

Bustamante, C., Marko, J.F., Siggia, E.D., and Smith, S. (1994). Entropic elasticity of lambda-phage DNA. Science *265*, 1599–1600.

Bustamante, C., Macosko, J.C., and Wuite, G.J. (2000). Grabbing the cat by the tail: manipulating molecules one by one. Nat. Rev. Mol. Cell Biol. *1*, 130–136.

Catalano, C.E. (2005). Viral genome packaging machines: An overview. In Viral Genome Packaging Machines: Genetics, Structure, and Mechanism, C.E. Catalano, ed. (New York: Kluwer/Plenum), pp. 1–4.

Chemla, Y.R., Aathavan, K., Michaelis, J., Grimes, S., Jardine, P.J., Anderson, D.L., and Bustamante, C. (2005). Mechanism of force generation of a viral DNA packaging motor. Cell *122*, 683–692.

Cheng, W., Dumont, S., Tinoco, I., Jr., and Bustamante, C. (2007). NS3 helicase actively separates RNA strands and senses sequence barriers ahead of the opening fork. Proc. Natl. Acad. Sci. USA *104*, 13954–13959.

Cornish, P.V., Ermolenko, D.N., Noller, H.F., and Ha, T. (2008). Spontaneous intersubunit rotation in single ribosomes. Mol. Cell *30*, 578–588.

Cornish, P.V., Ermolenko, D.N., Staple, D.W., Hoang, L., Hickerson, R.P., Noller, H.F., and Ha, T. (2009). Following movement of the L1 stalk between three functional states in single ribosomes. Proc. Natl. Acad. Sci. USA *106*, 2571–2576.

Dalal, R.V., Larson, M.H., Neuman, K.C., Gelles, J., Landick, R., and Block, S.M. (2006). Pulling on the nascent RNA during transcription does not alter kinetics of elongation or ubiquitous pausing. Mol. Cell *23*, 231–239.

Davenport, R.J., Wuite, G.J., Landick, R., and Bustamante, C. (2000). Single-molecule study of transcriptional pausing and arrest by E. coli RNA polymerase. Science *287*, 2497–2500.

Depken, M., Galburt, E.A., and Grill, S.W. (2009). The origin of short transcriptional pauses. Biophys. J. *96*, 2189–2193.

Dessinges, M.N., Lionnet, T., Xi, X.G., Bensimon, D., and Croquette, V. (2004). Single-molecule assay reveals strand switching and enhanced processivity of UvrD. Proc. Natl. Acad. Sci. USA *101*, 6439–6444.

Dhar, A., and Feiss, M. (2005). Bacteriophage lambda terminase: alterations of the high-affinity ATPase affect viral DNA packaging. J. Mol. Biol. *347*, 71–80.

Dohoney, K.M., and Gelles, J. (2001). Chi-sequence recognition and DNA translocation by single RecBCD helicase/nuclease molecules. Nature *409*, 370–374.

Doublie, S., Tabor, S., Long, A.M., Richardson, C.C., and Ellenberger, T. (1998). Crystal structure of a bacteriophage T7 DNA replication complex at 2.2 A resolution. Nature *391*, 251–258.

Dumont, S., Cheng, W., Serebrov, V., Beran, R.K., Tinoco, I., Jr., Pyle, A.M., and Bustamante, C. (2006). RNA translocation and unwinding mechanism of HCV NS3 helicase and its coordination by ATP. Nature *439*, 105–108.

Enemark, E.J., and Joshua-Tor, L. (2008). On helicases and other motor proteins. Curr. Opin. Struct. Biol. *18*, 243–257.

Ermolenko, D.N., Majumdar, Z.K., Hickerson, R.P., Spiegel, P.C., Clegg, R.M., and Noller, H.F. (2007). Observation of intersubunit movement of the ribosome in solution using FRET. J. Mol. Biol. *370*, 530–540.

Erzberger, J.P., and Berger, J.M. (2006). Evolutionary relationships and structural mechanisms of AAA+ proteins. Annu. Rev. Biophys. Biomol. Struct. *35*, 93–114.

Fei, J., Kosuri, P., MacDougall, D.D., and Gonzalez, R.L., Jr. (2008). Coupling of ribosomal L1 stalk and tRNA dynamics during translation elongation. Mol. Cell *30*, 348–359.

Finer, J.T., Simmons, R.M., and Spudich, J.A. (1994). Single myosin molecule mechanics: piconewton forces and nanometre steps. Nature *368*, 113–119.

Forde, N.R., Izhaky, D., Woodcock, G.R., Wuite, G.J., and Bustamante, C. (2002). Using mechanical force to probe the mechanism of pausing and arrest during continuous elongation by Escherichia coli RNA polymerase. Proc. Natl. Acad. Sci. USA *99*, 11682–11687.

Frank, J., Gao, H., Sengupta, J., Gao, N., and Taylor, D.J. (2007). The process of mRNA-tRNA translocation. Proc. Natl. Acad. Sci. USA *104*, 19671–19678.

Frick, D.N. (2003). Helicases as antiviral drug targets. Drug News Perspect. *16*, 355–362.

Fuller, D.N., Raymer, D.M., Kottadiel, V.I., Rao, V.B., and Smith, D.E. (2007a). Single phage T4 DNA packaging motors exhibit large force generation, high velocity, and dynamic variability. Proc. Natl. Acad. Sci. USA *104*, 16868–16873.

Fuller, D.N., Raymer, D.M., Rickgauer, J.P., Robertson, R.M., Catalano, C.E., Anderson, D.L., Grimes, S., and Smith, D.E. (2007b). Measurements of single DNA molecule packaging dynamics in bacteriophage lambda reveal high forces, high motor processivity, and capsid transformations. J. Mol. Biol. *373*, 1113–1122.

Galburt, E.A., Grill, S.W., Wiedmann, A., Lubkowska, L., Choy, J., Nogales, E., Kashlev, M., and Bustamante, C. (2007). Backtracking determines the force sensitivity of RNAP II in a factor-dependent manner. Nature *446*, 820–823.

Gangloff, S., Soustelle, C., and Fabre, F. (2000). Homologous recombination is responsible for cell death in the absence of the Sgs1 and Srs2 helicases. Nat. Genet. *25*, 192–194.

Gorbalenya, A.E., and Koonin, E.V. (1993). Helicases: amino acid sequence comparisons and structure-function relationships. Curr. Opin. Struct. Biol. *3*, 419–429.

Grimes, S., and Anderson, D. (1997a). The bacteriophage phi29 packaging proteins supercoil the DNA ends. J. Mol. Biol. *266*, 901–914.

Grimes, S., and Anderson, D. (1997b). The bacteriophage phi 29 packaging proteins supercoil the DNA ends. J. Mol. Biol. *266*, 901–914.

Grimes, S., Jardine, P.J., and Anderson, D. (2002). Bacteriophage phi 29 DNA packaging. Adv. Virus Res. *58*, 255–294.

Ha, T., Rasnik, I., Cheng, W., Babcock, H.P., Gauss, G.H., Lohman, T.M., and Chu, S. (2002). Initiation and re-initiation of DNA unwinding by the Escherichia coli Rep helicase. Nature *419*, 638–641.

Hamdan, S.M., Loparo, J.J., Takahashi, M., Richardson, C.C., and van Oijen, A.M. (2009). Dynamics of DNA replication loops reveal temporal control of lagging-strand synthesis. Nature *457*, 336–339.

Hell, S.W. (2007). Far-field optical nanoscopy. Science *316*, 1153–1158.

Herbert, K.M., La Porta, A., Wong, B.J., Mooney, R.A., Neuman, K.C., Landick, R., and Block, S.M. (2006). Sequence-resolved detection of pausing by single RNA polymerase molecules. Cell *125*, 1083–1094.

Hodges, C., Bintu, L., Lubkowska, L., Kashlev, M., and Bustamante, C. (2009). Nucleosomal fluctuations govern the transcription dynamics of RNA polymerase II. Science *325*, 626–628.

Hohng, S., Zhou, R., Nahas, M.K., Yu, J., Schulten, K., Lilley, D.M., and Ha, T. (2007). Fluorescence-force spectroscopy maps two-dimensional reaction landscape of the holliday junction. Science *318*, 279–283.

Huang, B., Wang, W., Bates, M., and Zhuang, X. (2008). Three-dimensional super-resolution imaging by stochastic optical reconstruction microscopy. Science *319*, 810–813.

Ibarra, B., Chemla, Y.R., Plyasunov, S., Smith, S.B., Lazaro, J.M., Salas, M., and Bustamante, C. (2009). Proofreading dynamics of a processive DNA polymerase. EMBO J. *28*, 2794–2802.

Ishijima, A., Kojima, H., Funatsu, T., Tokunaga, M., Higuchi, H., Tanaka, H., and Yanagida, T. (1998). Simultaneous observation of individual ATPase and mechanical events by a single myosin molecule during interaction with actin. Cell *92*, 161–171.

Iyer, L.M., Leipe, D.D., Koonin, E.V., and Aravind, L. (2004a). Evolutionary history and higher order classification of AAA+ ATPases. J. Struct. Biol. *146*, 11–31.

Iyer, L.M., Makarova, K.S., Koonin, E.V., and Aravind, L. (2004b). Comparative genomics of the FtsK-HerA superfamily of pumping ATPases: implications for the origins of chromosome segregation, cell division and viral capsid packaging. Nucleic Acids Res. *32*, 5260–5279.

Jankowsky, E., and Bowers, H. (2006). Remodeling of ribonucleoprotein complexes with DExH/D RNA helicases. Nucleic Acids Res. *34*, 4181–4188.

Jardine, P.J., and Anderson, D. (2006). DNA packaging in double-stranded DNA bacteriophages. In The Bacteriophages, R. Calendar, ed. (New York: Oxford University Press), pp. 49–65.

Jennings, T.A., Mackintosh, S.G., Harrison, M.K., Sikora, D., Sikora, B., Dave, B., Tackett, A.J., Cameron, C.E., and Raney, K.D. (2009). NS3 helicase from the hepatitis C virus can function as a monomer or oligomer depending on enzyme and substrate concentrations. J. Biol. Chem. *284*, 4806–4814.

Jin, J., Bai, L., Johnson, D.S., Fulbright, R.M., Kireeva, M.L., Kashlev, M., and Wang, M.D. (2010). Synergistic action of RNA polymerases in overcoming the nucleosomal barrier. Nat. Struct. Mol. Biol. *17*, 745–752.

Johnson, D.S., Bai, L., Smith, B.Y., Patel, S.S., and Wang, M.D. (2007). Single-molecule studies reveal dynamics of DNA unwinding by the ring-shaped T7 helicase. Cell *129*, 1299–1309.

Julian, P., Konevega, A.L., Scheres, S.H., Lazaro, M., Gil, D., Wintermeyer, W., Rodnina, M.V., and Valle, M. (2008). Structure of ratcheted ribosomes with tRNAs in hybrid states. Proc. Natl. Acad. Sci. USA *105*, 16924–16927.

Kapanidis, A.N., Margeat, E., Laurence, T.A., Doose, S., Ho, S.O., Mukhopadhyay, J., Kortkhonjia, E., Mekler, V., and Ebright, R.H. (2005). Retention of transcription initiation factor σ^{70} in transcription elongation: Single-molecule analysis. Mol. Cell *20*, 347–356.

Kapanidis, A.N., Margeat, E., Ho, S.O., Kortkhonjia, E., Weiss, S., and Ebright, R.H. (2006). Initial transcription by RNA polymerase proceeds through a DNA-scrunching mechanism. Science *314*, 1144–1147.

Keller, D., and Bustamante, C. (2000). The mechanochemistry of molecular motors. Biophys. J. *78*, 541–556.

Kolykhalov, A.A., Mihalik, K., Feinstone, S.M., and Rice, C.M. (2000). Hepatitis C virus-encoded enzymatic activities and conserved RNA elements in the 3′ nontranslated region are essential for virus replication in vivo. J. Virol. *74*, 2046–2051.

Koonin, E.V., Senkevich, T.G., and Chernos, V.I. (1993). Gene A32 product of vaccinia virus may be an ATPase involved in viral DNA packaging as indicated by sequence comparisons with other putative viral ATPases. Virus Genes *7*, 89–94.

Korolev, S., Yao, N., Lohman, T.M., Weber, P.C., and Waksman, G. (1998). Comparisons between the structures of HCV and Rep helicases reveal structural similarities between SF1 and SF2 super-families of helicases. Protein Sci. *7*, 605–610.

Koti, J.S., Morais, M.C., Rajagopal, R., Owen, B.A., McMurray, C.T., and Anderson, D.L. (2008). DNA packaging motor assembly intermediate of bacteriophage phi29. J. Mol. Biol. *381*, 1114–1132.

Krejci, L., Van Komen, S., Li, Y., Villemain, J., Reddy, M.S., Klein, H., Ellenberger, T., and Sung, P. (2003). DNA helicase Srs2 disrupts the Rad51 presynaptic filament. Nature *423*, 305–309.

Lam, A.M., and Frick, D.N. (2006). Hepatitis C virus subgenomic replicon requires an active NS3 RNA helicase. J. Virol. *80*, 404–411.

Lang, M.J., Fordyce, P.M., Engh, A.M., Neuman, K.C., and Block, S.M. (2004). Simultaneous, coincident optical trapping and single-molecule fluorescence. Nat. Methods *1*, 133–139.

Larson, M.H., Greenleaf, W.J., Landick, R., and Block, S.M. (2008). Applied force reveals mechanistic and energetic details of transcription termination. Cell *132*, 971–982.

Lee, T.H., Blanchard, S.C., Kim, H.D., Puglisi, J.D., and Chu, S. (2007). The role of fluctuations in tRNA selection by the ribosome. Proc. Natl. Acad. Sci. USA *104*, 13661–13665.

Lehman, I.R., Bessman, M.J., Simms, E.S., and Kornberg, A. (1958). Enzymatic synthesis of deoxyribonucleic acid. I. Preparation of substrates and partial purification of an enzyme from Escherichia coli. J. Biol. Chem. *233*, 163–170.

Liljas, A. (2004). Structural Aspects of Protein Synthesis (Singapore: World Scientific Publishing Co.).

Lindenbach, B.D., and Rice, C.M. (2005). Unravelling hepatitis C virus replication from genome to function. Nature *436*, 933–938.

Lionnet, T., Spiering, M.M., Benkovic, S.J., Bensimon, D., and Croquette, V. (2007). Real-time observation of bacteriophage T4 gp41 helicase reveals an unwinding mechanism. Proc. Natl. Acad. Sci. USA *104*, 19790–19795.

Liu, S., Abbondanzieri, E.A., Rausch, J.W., Le Grice, S.F., and Zhuang, X. (2008). Slide into action: dynamic shuttling of HIV reverse transcriptase on nucleic acid substrates. Science *322*, 1092–1097.

Lohman, T.M., and Bjornson, K.P. (1996). Mechanisms of helicase-catalyzed DNA unwinding. Annu. Rev. Biochem. *65*, 169–214.

Lohman, T.M., Thorn, K., and Vale, R.D. (1998). Staying on track: Common features of DNA helicases and microtubule motors. Cell *93*, 9–12.

Lohman, T.M., Tomko, E.J., and Wu, C.G. (2008). Non-hexameric DNA helicases and translocases: mechanisms and regulation. Nat. Rev. Mol. Cell Biol. *9*, 391–401.

Ma, Y., Yates, J., Liang, Y., Lemon, S.M., and Yi, M. (2008). NS3 helicase domains involved in infectious intracellular hepatitis C virus particle assembly. J. Virol. *82*, 7624–7639.

Mackintosh, S.G., and Raney, K.D. (2006). DNA unwinding and protein displacement by superfamily 1 and superfamily 2 helicases. Nucleic Acids Res. *34*, 4154–4159.

Margeat, E., Kapanidis, A.N., Tinnefeld, P., Wang, Y., Mukhopadhyay, J., Ebright, R.H., and Weiss, S. (2006). Direct observation of abortive initiation and promoter escape within single immobilized transcription complexes. Biophys. J. *90*, 1419–1431.

Marshall, R.A., Aitken, C.E., Dorywalska, M., and Puglisi, J.D. (2008). Translation at the single-molecule level. Annu. Rev. Biochem. *77*, 177–203.

Matson, S.W., Bean, D.W., and George, J.W. (1994). DNA helicases: enzymes with essential roles in all aspects of DNA metabolism. Bioessays *16*, 13–22.

Mejia, Y.X., Mao, H., Forde, N.R., and Bustamante, C. (2008). Thermal probing of E. coli RNA polymerase off-pathway mechanisms. J. Mol. Biol. *382*, 628–637.

Mitchell, M.S., Matsuzaki, S., Imai, S., and Rao, V.B. (2002). Sequence analysis of bacteriophage T4 DNA packaging/terminase genes 16 and 17 reveals a common ATPase center in the large subunit of viral terminases. Nucleic Acids Res. *30*, 4009–4021.

Moffitt, J.R., Chemla, Y.R., Izhaky, D., and Bustamante, C. (2006). Differential detection of dual traps improves the spatial resolution of optical tweezers. Proc. Natl. Acad. Sci. USA *103*, 9006–9011.

Moffitt, J.R., Chemla, Y.R., Aathavan, K., Grimes, S., Jardine, P.J., Anderson, D.L., and Bustamante, C. (2009). Intersubunit coordination in a homomeric ring ATPase. Nature *457*, 446–450.

Moore, P.B., and Steitz, T.A. (2003). The structural basis of large ribosomal subunit function. Annu. Rev. Biochem. *72*, 813–850.

Moradpour, D., Penin, F., and Rice, C.M. (2007). Replication of hepatitis C virus. Nat. Rev. Microbiol. *5*, 453–463.

Morais, M.C., Koti, J.S., Bowman, V.D., Reyes-Aldrete, E., Anderson, D.L., and Rossmann, M.G. (2008). Defining molecular and domain boundaries in the bacteriophage phi29 DNA packaging motor. Structure *16*, 1267–1274.

Murakami, A., Ishida, S., and Dickson, C. (2002). GATA-4 interacts distinctively with negative and positive regulatory elements in the Fgf-3 promoter. Nucleic Acids Res. *30*, 1056–1064.

Muschielok, A., Andrecka, J., Jawhari, A., Bruckner, F., Cramer, P., and Michaelis, J. (2008). A nano-positioning system for macromolecular structural analysis. Nat. Methods *5*, 965–971.

Myong, S., and Ha, T. (2010). Stepwise translocation of nucleic acid motors. Curr. Opin. Struct. Biol. *20*, 121–127.

Myong, S., Rasnik, I., Joo, C., Lohman, T.M., and Ha, T. (2005). Repetitive shuttling of a motor protein on DNA. Nature *437*, 1321–1325.

Myong, S., Bruno, M.M., Pyle, A.M., and Ha, T. (2007). Spring-loaded mechanism of DNA unwinding by hepatitis C virus NS3 helicase. Science *317*, 513–516.

Neuman, K.C., Abbondanzieri, E.A., Landick, R., Gelles, J., and Block, S.M. (2003). Ubiquitous transcriptional pausing is independent of RNA polymerase backtracking. Cell *115*, 437–447.

Nudler, E., Mustaev, A., Lukhtanov, E., and Goldfarb, A. (1997). The RNA-DNA hybrid maintains the register of transcription by preventing backtracking of RNA polymerase. Cell *89*, 33–41.

Ogawa, T., and Okazaki, T. (1980). Discontinuous DNA replication. Annu. Rev. Biochem. *49*, 421–457.

Palladino, F., and Klein, H.L. (1992). Analysis of mitotic and meiotic defects in Saccharomyces cerevisiae SRS2 DNA helicase mutants. Genetics *132*, 23–37.

Pang, P.S., Jankowsky, E., Planet, P.J., and Pyle, A.M. (2002). The hepatitis C viral NS3 protein is a processive DNA helicase with cofactor enhanced RNA unwinding. EMBO J. *21*, 1168–1176.

Park, J., Myong, S., Niedziela-Majka, A., Yu, J., Lohman, T.M., and Ha, T. (2010). PcrA helicase dismantles RecA filaments by reeling in DNA in uniform steps. Cell *142*, 1–12.

Patel, S.S., and Picha, K.M. (2000). Structure and function of hexameric helicases. Annu. Rev. Biochem. *69*, 651–697.

Pyle, A.M. (2008). Translocation and unwinding mechanisms of RNA and DNA helicases. Annu. Rev. Biophys. *37*, 317–336.

Ramakrishnan, V. (2002). Ribosome structure and the mechanism of translation. Cell *108*, 557–572.

Raney, K.D., Sharma, S.D., Moustafa, I.M., and Cameron, C.E. (2010). Hepatitis C virus non-structural protein 3 (HCV NS3): a multifunctional antiviral target. J. Biol. Chem. *285*, 22725–22731.

Rao, V.B., and Feiss, M. (2008). The bacteriophage DNA packaging motor. Annu. Rev. Genet. *42*, 647–681.

Revyakin, A., Liu, C., Ebright, R.H., and Strick, T.R. (2006). Abortive initiation and productive initiation by RNA polymerase involve DNA scrunching. Science *314*, 1139–1143.

Rickgauer, J.P., Fuller, D.N., Bo, H., Grimes, S., Jardine, P.J., Anderson, D.L., and Smith, D.E. (2006). Initiation of bacteriophage phi 29 DNA packaging studied by optical tweezers manipulation of single DNA molecules. Proceedings of the SPIE - The International Society for Optical Engineering, 632623-632621-632628.

Rivetti, C., Guthold, M., and Bustamante, C. (1999). Wrapping of DNA around the E.coli RNA polymerase open promoter complex. EMBO J. *18*, 4464–4475.

Rocak, S., and Linder, P. (2004). DEAD-box proteins: the driving forces behind RNA metabolism. Nat. Rev. Mol. Cell Biol. *5*, 232–241.

Saha, A., Wittmeyer, J., and Cairns, B.R. (2006). Chromatin remodelling: the industrial revolution of DNA around histones. Nat. Rev. Mol. Cell Biol. *7*, 437–447.

Serebrov, V., and Pyle, A.M. (2004). Periodic cycles of RNA unwinding and pausing by hepatitis C virus NS3 helicase. Nature *430*, 476–480.

Serebrov, V., Beran, R.K., and Pyle, A.M. (2009). Establishing a mechanistic basis for the large kinetic steps of the NS3 helicase. J. Biol. Chem. *284*, 2512–2521.

Shaevitz, J.W., Abbondanzieri, E.A., Landick, R., and Block, S.M. (2003). Backtracking by single RNA polymerase molecules observed at near-base-pair resolution. Nature *426*, 684–687.

Shiratori, A., Shibata, T., Arisawa, M., Hanaoka, F., Murakami, Y., and Eki, T. (1999). Systematic identification, classification, and characterization of the open reading frames which encode novel helicase-related proteins in Saccharomyces cerevisiae by gene disruption and Northern analysis. Yeast *15*, 219–253.

Smith, D.E., Tans, S.J., Smith, S.B., Grimes, S., Anderson, D.L., and Bustamante, C. (2001). The bacteriophage straight phi29 portal motor can package DNA against a large internal force. Nature *413*, 748–752.

Smith, S.B., Finzi, L., and Bustamante, C. (1992). Direct mechanical measurements of the elasticity of single DNA molecules by using magnetic beads. Science *258*, 1122–1126.

Smith, S.B., Cui, Y., and Bustamante, C. (1996). Overstretching B-DNA: the elastic response of individual double-stranded and single-stranded DNA molecules. Science *271*, 795–799.

Stano, N.M., Jeong, Y.J., Donmez, I., Tummalapalli, P., Levin, M.K., and Patel, S.S. (2005). DNA synthesis provides the driving force to accelerate DNA unwinding by a helicase. Nature *435*, 370–373.

Sternberg, S.H., Fei, J.Y., Prywes, N., McGrath, K.A., and Gonzalez, R.L. (2009). Translation factors direct intrinsic ribosome dynamics during translation termination and ribosome recycling. Nat. Struct. Mol. Biol. *16*, 861–888.

Story, R.M., Weber, I.T., and Steitz, T.A. (1992). The structure of the E. coli recA protein monomer and polymer. Nature *355*, 318–325.

Straney, D.C., and Crothers, D.M. (1987). A stressed intermediate in the formation of stably initiated RNA chains at the Escherichia coli lac UV5 promoter. J. Mol. Biol. *193*, 267–278.

Strick, T.R., Allemand, J.F., Bensimon, D., Bensimon, A., and Croquette, V. (1996). The elasticity of a single supercoiled DNA molecule. Science *271*, 1835–1837.

Thomsen, N.D., and Berger, J.M. (2008). Structural frameworks for considering microbial protein- and nucleic acid-dependent motor ATPases. Mol. Microbiol. *69*, 1071–1090.

Tsay, J.M., Sippy, J., Feiss, M., and Smith, D.E. (2009). The Q motif of a viral packaging motor governs its force generation and communicates ATP recognition to DNA interaction. Proc. Natl. Acad. Sci. USA *106*, 14355–14360.

Tsay, J.M., Sippy, J., DelToro, D., Andrews, B.T., Draper, B., Rao, V., Catalano, C.E., Feiss, M., and Smith, D.E. (2010). Mutations altering a structurally conserved loop-helix-loop region of a viral packaging motor change DNA translocation velocity and processivity. J. Biol. Chem. *285*, 24282–24289.

Turnquist, S., Simon, M., Egelman, E., and Anderson, D. (1992). Supercoiled DNA wraps around the bacteriophage phi 29 head-tail connector. Proc. Natl. Acad. Sci. USA *89*, 10479–10483.

Uemura, S., Dorywalska, M., Lee, T.H., Kim, H.D., Puglisi, J.D., and Chu, S. (2007). Peptide bond formation destabilizes Shine-Dalgarno interaction on the ribosome. Nature *446*, 454–457.

Uemura, S., Aitken, C.E., Korlach, J., Flusberg, B.A., Turner, S.W., and Puglisi, J.D. (2010). Real-time tRNA transit on single translating ribosomes at codon resolution. Nature *464*, 1012–1017.

Veaute, X., Jeusset, J., Soustelle, C., Kowalczykowski, S.C., Le Cam, E., and Fabre, F. (2003). The Srs2 helicase prevents recombination by disrupting Rad51 nucleoprotein filaments. Nature *423*, 309–312.

Visscher, K., Schnitzer, M.J., and Block, S.M. (1999). Single kinesin molecules studied with a molecular force clamp. Nature *400*, 184–189.

Waksman, G., Lanka, E., and Carazo, J.M. (2000). Helicases as nucleic acid unwinding machines. Nat. Struct. Biol. *7*, 20–22.

Walter, W., Kireeva, M.L., Studitsky, V.M., and Kashlev, M. (2003). Bacterial polymerase and yeast polymerase II use similar mechanisms for transcription through nucleosomes. J. Biol. Chem. *278*, 36148–36156.

Wang, M.D., Schnitzer, M.J., Yin, H., Landick, R., Gelles, J., and Block, S.M. (1998). Force and velocity measured for single molecules of RNA polymerase. Science *282*, 902–907.

Wen, J.D., Lancaster, L., Hodges, C., Zeri, A.C., Yoshimura, S.H., Noller, H.F., Bustamante, C., and Tinoco, I. (2008). Following translation by single ribosomes one codon at a time. Nature *452*, 598–603.

Worrall, J.A., Howe, F.S., McKay, A.R., Robinson, C.V., and Luisi, B.F. (2008). Allosteric activation of the ATPase activity of the Escherichia coli RhlB RNA helicase. J. Biol. Chem. *283*, 5567–5576.

Wu, J.Y., Stone, M.D., and Zhuang, X. (2010). A single-molecule assay for telomerase structure-function analysis. Nucleic Acids Res. *38*, e16.

Wuite, G.J., Smith, S.B., Young, M., Keller, D., and Bustamante, C. (2000). Single-molecule studies of the effect of template tension on T7 DNA polymerase activity. Nature *404*, 103–106.

Yildiz, A., Forkey, J.N., McKinney, S.A., Ha, T., Goldman, Y.E., and Selvin, P.R. (2003). Myosin V walks hand-over-hand: single fluorophore imaging with 1.5-nm localization. Science *300*, 2061–2065.

Yin, H., Wang, M.D., Svoboda, K., Landick, R., Block, S.M., and Gelles, J. (1995). Transcription against an applied force. Science *270*, 1653–1657.